"This is the peer reviewed version of the following article: [Smith TD, CJ Bonar. 2022. Nasal anatomy of agoutis (Dasyprocta spp.). Vertebrate Zoology 72: 95-113. <u>DOI:</u> 10.3897/vz.72.e76047], which has been published in final form at [Link to final article using the DOI]. This article may be used for non-commercial purposes in accordance with Wiley Terms and Conditions for Use of Self-Archived Versions."

The nasal cavity in agoutis (*Dasyprocta* spp.): a micro-computed tomographic and histological study

Timothy D. Smith¹, Christopher J. Bonar²

1 School of Physical Therapy, Slippery Rock University, Slippery Rock, PA 16057, USA

2 Franklin Park Zoo, One Franklin Park Road, Boston, MA 02121, USA

Corresponding author: Tim D. Smith (timothy.smith@sru.edu)

Academic editor Irina Ruf Received 02 October 2021 Accepted 31 January 2022 Published 21 February 2022

Citation: Smith TD, Bonar CJ (2022) The nasal cavity in agoutis (*Dasyprocta* spp.): a microcomputed tomographic and histological study. Vertebrate Zoology 72:95-113. https://10.3897/vz.72.e76047

Abstract

Nasal anatomy in rodents is well-studied, but most current knowledge is based on small-bodied muroid species. Nasal anatomy and histology of hystricognaths, the largest living rodents, remains poorly understood. Here, we describe the nasal cavity of agoutis (Dasyprocta spp.), the first large-bodied South American rodents to be studied histologically throughout the nasal cavity. Two adult agoutis were studied using microcomputed tomography, and in one of these, half the snout was serially sectioned and stained for microscopic study. Certain features are notable in *Dasyprocta*. The frontal recess has five turbinals within it, the most in this space compared to other rodents that have been studied. The nasoturbinal is particularly large in dorsoventral and rostrocaudal dimensions and is entirely non-olfactory in function, in apparent contrast to known muroids. Whether this relates solely to body size scaling or perhaps also relates to directing airflow or conditioning inspired air requires further study. In addition, olfactory epithelium appears more restricted to the olfactory and frontal recesses compared to muroids. At the same time, the rostral tips of the olfactory turbinals bear at least some nonolfactory epithelium. The findings of this study support the hypothesis that turbinals are multifunctional structures, indicating investigators should use caution when categorizing turbinals as specialized for one function (e.g., olfaction or respiratory air-conditioning). Caution may be especially appropriate in the case of large-bodied mammals, in which the different scaling characteristics of respiratory and olfactory mucosa result in relative more of the former type as body size increases.

Key Words

craniofacial, paranasal, Rodentia, turbinal, turbinate

Introduction

Among mammals, nasal histology is perhaps best studied in rodents. Many rodents represent ideal candidates for histological study by virtue of their small body size. Previously, the nasal fossa has been histologically studied and quantified in at least six rodents, including the laboratory mouse (Mus musculus) and rat (Rattus norvegicus), hamster (Mesocricetus auratus), voles (Microtus gregalis, Myodes sp.), deer mouse (Peromyscus maniculatus), and gray squirrel (Sciurus carolinensis) (Gurtovoi, 1966; Adams, 1972; Gross et al., 1982; Clancy et al., 1994; Barrios et al., 2014). Many more rodents have been studied and quantified osteologically, analyzing bones as proxies for olfactory or respiratory physiology (Martinez et al., 2018, 2020). These studies, in combination with other published data, reveal that rodents, along with eulipotyphlans and some other small mammals, have relatively large olfactory surface area (for their body size) compared a diverse array of mammals (Smith et al., 2014; Yee et al., 2016). In addition, these studies reveal common characteristics of nasal structures in rodents. For instance, turbinals of the ethmoid bone (including ethmoturbinals, frontoturbinals, and the nasoturbinal) bear the majority of olfactory mucosa within the rodent nasal fossa (Adams, 1972; Yee et al., 2016). Olfactory epithelium is notably the predominant type with recesses that exist as *culs-de*sac in the dorsocaudal region of the nasal fossa. However, ethmoturbinals that project rostral to these recesses, and portions of the nasoturbinal, are also lined by at least some olfactory epithelium (Adams, 1972; Yee et al., 2016).

Rodents also are common models for computational fluid dynamics of nasal airflow. Studies using laboratory rats reveal that there are spatially distinct streams of nasal airflow: a more ventral stream associated with ventral structures and spaces (maxilloturbinal rostrally and the nasopharyngeal ducts caudally) and more dorsal, lateral, and medial streams which fan across more other turbinals which bear much olfactory epithelium (Kimbell et al., 1997; Jiang and Zhao, 2010). Some variations in airflow do occur with altered inspiratory patterns (e.g., "sniffing;" Zhao et al., 2006). However, segregation of airstreams has been observed in rodents (Jiang and Zhao, 2010) and canids (Craven et al., 2009, 2010; Lawson et al., 2012), mammals thought of as olfactory specialists. Craven et al. (2010) considered the combined characteristics of a dedicated olfactory space (the aforementioned dorsocaudal recesses) and dedicated olfactory and respiratory airstreams to be defining characteristics of "macrosmatic" mammals, or those specialized for optimized olfactory function.

Rodent nasal anatomy and histology

Here, we employ terminology rooted in nasal cavity development (described below), with a lengthy history of usage (e.g., see Maier, 1993a, b; Maier and Ruf, 2014). Using this developmental terminology, Ruf (2020) thoroughly discussed the prenatal nasal "template" (or cartilaginous nasal capsule) as well as the adult skeletal anatomy of muroid rodents. All muroids possess a nasoturbinal, a maxilloturbinal, and three ethmoturbinals (or four, depending on

convention; see below); these are named based on their bony articulation in adults, although they all originate from the fetal cartilaginous capsule (Maier, 1993a, b). This arrangement is found in many mammals of other orders, including most non anthropoid primates (Kollmann and Papin, 1925; Smith and Rossie, 2008; Smith et al., 2019; Lundeen and Kirk, 2019), scandentians (Wible, 2011), lagomorphs (Negus, 1958; Ruf, 2014) and many carnivorans (Negus, 1958; Van Valkenburgh et al., 2014a). Given the frequency of this arrangement concerning the larger turbinals that project close to the nasal septum, this arrangement may be a plesiomorphic for mammals (but see Lundeen and Kirk, 2019). However, we have less clarity in comparative anatomy of smaller "accessory" turbinals that grow between larger turbinals, or are tucked in recesses, and thus are more difficult to observe grossly (sometimes called "ectoturbinals," but see Van Valkenburgh et al. 2014b, regarding problematic issue of this term).

Regarding adult rodent nasal anatomy, monographic works such as that by Dieulafé (1906) and Negus (1958) offer surprising little detail. In describing rodents (based on rat and guinea pig), Dieulafé (1906) is more detailed than Negus (1958). He describes the maxilloturbinal as having only one upwardly directed "roll." He describes the nasoturbinal in *Cavia* as a lamina (with no scrolling) covering the superior border of the maxilloturbinal; it is rostrocaudally coextensive with the maxilloturbinal in *Cavia*. In *Rattus*, he describes the nasoturbinal to be rostrocaudally less extensive than the maxilloturbinal. Dieulafé numbers three ethmoturbinals in *Cavia* and four in *Rattus*. However, Kelemen (1950) describes four ethmoturbinals in *Cavia*. To an extent, these and other discrepancies have arisen due to terminological practices that have differed among researchers. However, there are some references suggesting variation. For example, Moore (1981, citing Paulli) noted the African porcupine (*Hystrix cristata*) has an extra ethmoturbinals (in Moore, "endoturbinal").

Behavioral, experimental, and genetic evidence support the idea that rodents do indeed possess olfactory capabilities that are relatively advanced compared to some other mammals (Rouquier et al., 2000; Laska et al., 2005) with some variation based on ecological variables (e.g., Vander Wall et al., 2003). However, given that rodents are the most speciose mammalian order (with more than 2600 species, D'Elía et al. 2019), nasal anatomy has not been studied equally in across all groups. Whereas certain nasal structures have been examined more broadly, such as the vomeronasal organ (e.g., Weiler et al., 1999; Smith et al., 2001, 2007; Torres et al., 2020) or rostral nasal cartilages (e.g., Maier and Schrenk; 1987; Mess, 1999), the entirety of the nasal cavity has been examined in a narrow range of rodents, and mostly myomorphans (e.g., Ruf, 2020). Even less is known about distribution of olfactory and respiratory mucosa within the nasal cavities. In mammals broadly, the turbinals that reside or project most rostrally are covered entirely (i.e., maxilloturbinal) or at least partially (e.g., nasoturbinal and first ethmoturbinal) by respiratory epithelium. Conversely, those turbinals that are sequestered in the olfactory recess are typically covered mostly by olfactory epithelium (e.g., Adams, 1972; Smith and Rossie, 2008; Yee et al., 2016; Smith et al., 2019). Within Rodentia, we have only limited knowledge. In a recent appraisal of the literature on nasal epithelial distribution, Yee et al. (2016) summarize data on 27 mammals, five of which are rodents. Yet, all five are muroid species.

There are practical reasons for the limited scope of our knowledge on rodent nasal anatomy. For example, rodents vary in body size from 3.75 g to 50 kg, with the smallest rodent being a muroid species (Boël et al., 2020; MacDonald et al., 2013). Many larger taxa, such as New World hystricomorphans are understudied because of the challenges in studying large mammals by histology. Large specimens present special challenges for histological methods due to greater distortion (e.g., DeLeon and Smith, 2014), size-related limitations that necessitate trimming of portions of nasal tissues, or dividing into multiple blocks (Smith et 1., 2021) or preservation issues (Yee et al., 2016) compared to the study of smaller species. Thus, while recent work has greatly expanded the scope of our microanatomical knowledge of smaller-bodied rodents such as muroids (Ruf, 2020), our knowledge of larger-bodied rodents is greatly limited. The largest rodent for which nasal anatomy has been studied by histology is the chinchilla (Jurcisek et al., 2003). Chinchillas are one of the New World groups in the infraorder Hystricognathi, a diverse group of rodents including some of the largest (e.g., porcupines, capybara) and most unusual (mole rats) species. At ~ 700 g body mass, the chinchilla (*Chinchilla lanigera*) is one of the smaller hystricognaths. Examination of a wider range of rodents in the infraorder may clarify how internal nasal structures vary relative to body size variation in rodents.

In the present study we address this imbalance in our knowledge of rodents by examining the nasal fossa of agoutis, large-bodied South American cavioids. Agoutis (family Dasyproctidae) may weigh over 3 kg (Robinson and Redford, 1987). There is reason to expect variation among rodents regarding distribution of olfactory and respiratory epithelium along nasal surfaces. Previous work has shown that turbinals of the ethmoid bone (see below) vary extensively across mammals in the amount of olfactory and non-olfactory epithelium (Smith et al., 2007, 2019; Pang et al., 2016; Yee et al., 2016). Accordingly, without adequate histological data, it is difficult to employ osseous structures as functional proxies without some microanatomical knowledge of their mucosal coverings (see further discussion in Smith et al., 2007; Van Valkenburgh et al., 2014b; Pang et al., 2016; Yee et al., 2016). Thus, our primary aim is to assess the total number and microanatomical characteristics of turbinals and other bony structures within the nasal fossa in the agouti, and to contrast this with previous descriptions of other rodents.

Methods

Sample

Individuals in the cadaveric sample used in this study were obtained after death by natural causes in at the Cleveland Metroparks Zoo. Each specimen was fixed in 10% buffered formalin by immersion. One was a 7-year-old female *Dasyrocta leporina* (red-rumped agouti) and the other was a 5-year-old female *Dasyprocta cristata* (crested agouti). The *D. cristata* was bisected with one half head used for histology 2.25 years after fixation. Subsequently, the remaining half head, plus the adult *D. leporina* were saved for further analysis, with periodic changes of formalin.

Histological and μ CT methods

Routine paraffin embedding followed decalcification in a formic acid-sodium citrate solution. Further details (concentration, weekly tests of completion etc.) of this solution were fully explained in DeLeon and Smith (2014). Sections were 12 µm thick, and every eighth section was mounted on glass slides. Slides were alternately stained using Gomori trichrome or hematoxylineosin procedures (for more details see DeLeon and Smith, 2014). Serial sections were examined by light microscopy using a Zeiss stereo microscope (X0.64 to X1.6 magnification) or a Leica DMLB photomicroscope (X25 to X630). Selected sections were photographed using an Axiocam MRc 5 Firewire camera attached to the Leica microscope) or an MRc 150 Firewire camera (attached to the Zeiss microscope).

Microcomputed tomography (μCT) was used to study the whole head of *D. leporina* and the half head of *D. cristata;* scanning for each head occurred approximately three years after fixation. μCT Scanning was conducted at Northeast Ohio Medical University using a Scanco vivaCT 75 scanner (scan parameters: 70 kVp; 114 mA). The volumes were reconstructed using 39 μm cubic voxels and exported as 8-bit TIFF stacks for three-dimensional reconstructions (DeLeon and Smith, 2014). TIFF stacks are publicly available at https://www.morphosource.org/projects/000398575?locale=en. All three-dimensional reconstructions were carried out using Amira ® 2019.1 software (Thermofisher).

Terminology of internal nasal structures

Universal agreement on nasal terminology appears unlikely, due to differing practices among many subdisciplines of anatomical sciences. However, individual authors can take pains to point to synonymous terms used to refer to particular structure, an effort we will undertake here. There are several systems of terminology for nasal cavity structures, requiring a brief discussion to clarify synonyms and thereby facilitate comparisons of our results with prior studies. Some of the terminology is human-centric; veterinary terminology bears some similarity to human terminology, but is more extensive due to greater complexity in the nose of most non-human mammals (Table 1). Some parallel terms easy to equate. For example, among inwardly scrolling bones in the nasal cavity, the inferior nasal concha is the same as the maxilloturbinal or maxilloturbinate (Table 1). But in other case there are no parallel terms due to evolutionary loss of much paranasal and dorsocaudal parts of the nasal template in humans, and anthropoid primates generally (Starck, 1975; Maier, 2000; Maier and Ruf, 2014; Smith et al., 2014).

The complexity of mammalian noses led to an intricate system of terms used by Paulli (1900) which categorized the most inwardly projecting scrolls as endoturbinals (endoturbinates) and more peripherally positioned turbinals as "ectoturbinals" (ectoturbinates). This system has been

widely used and popularized (e.g., Moore, 1981) and continues to be used (e.g., Pereira et al., 2020). A disadvantage of this terminology, as discussed elsewhere, is that these terms, in which turbinals are arbitrarily numbered beginning dorsomedially to ventrolaterally, make it very difficult to identify and compare homologous structures (see, Novacek, 1993; Smith and Rossie, 2008; Macrini, 2014; Maier and Ruf, 2014). Herein, we employ terminology deeply rooted in anatomical literature, based on development, and clearly articulated by Wolfgang Maier (Maier, 1993a, b). This terminology continues to be used with great frequency recently (e.g., Ruf, 2020; VanValkenburgh et al., 2014). In this system, turbinals are recognized in part based on the primary bone with which they articulate in adults (although they may articulate with more than one), and is also based on whether they form earlier or later in development. The so-called "endoturbinals" are thus recognized as the most inwardly projecting bones that, in the adult, primarily articulate with the maxilla (maxilloturbinal), nasal (nasoturbinal), or ethmoid (ethmoturbinals, variable in number). "Ectoturbinals" are instead called frontoturbinals if they develop within the frontal recess of the nasal capsule, or interturbinals if they are secondary, later developing turbinals that emerge between larger turbinals, but do not reach close to the midline (Table 1). The only deviation of our terminology from Maier (1993a) is that in our report, the second ethmoturbinal is equivalent to the posterior/ventral lamina of ethmoturbinal I as identified by other authors (Maier, 1993a; Ruf 2020). This preference in terminology is based on the initial (late embryological) separate appearance of the two lamellae, which later merge to a common root (Smith and Rossie, 2008). Additionally, recent work on bats has shown some species possess a small lamella emanating from the "ventral edge of the caudal part of ethmoturbinal I" (Ito et al., 2021, p. 11). Because the ventral projection the authors mention is both posterior and ventral to ethmoturbinal II (per our terminology), this finding potentially creates additional confusion for mammalian turbinal nomenclature denoting accessory lamellae. Nonetheless, terminology is likely to continue to vary until we better understand comparative mammalian development, so we include synonyms for ethmoturbinals in Fig. 1 (and see Table 1 for additional synonyms).

Other significant structures that are frequently discussed here include several plates or laminae. The horizontal lamina provides a lateral root of ethmoturbinal I, and at the same time separates the frontal and maxillary recesses. Rostrally, both of these recesses merge into a common cavity that goes by various names (Table 1), and here is called the anterolateral recess. The transverse lamina is an osseous plate composed partly of ethmoid and partly by the vomer, which separates an olfactory *cul-de-sac* space found dorsocaudally, from a dedicated respiratory airway (the nasopharyngeal duct) ventrally. The semicircular lamina (or crest) partially separates the more medial main nasal chamber, from the more lateral frontal recess.

Lastly, the term "recess itself" bears a distinguishing remark. Prior descriptions of paranasal spaces are also complicated by different terminological practices. Paranasal recesses as the peripheralized compartments that develop when the cartilaginous nasal capsule folds during prenatal development, a process called primary pneumatization (see Wang et al., 1994; Rossie, 2006). If, in the adult, these spaces remain proportionally similar to the fetal "template" for that recess, we retain the term recess (e.g., frontal recess). If secondarily, opportunistic osteoclastic

activity has excavated bone to change the shape of the recess, we consider this secondary pneumatization, and the term "sinus" (e.g., frontal sinus) is preferred (Witmer, 1997; Rossie, 2006; Smith et al., 2005). Without subadults to examine how the paranasal spaces change across age, we may not be able to identify the appropriate terminology in this report. However, comparative observations across rodents may shed some light on which terminology may be more accurate.

Results

Main nasal chamber

The *Dasyprocta leporina* specimen permitted a basic osteological description of the nasal cavity. In terms to osseous structures, the main chamber of the nasal fossa spans the distance from the ventral limit of the piriform aperture to the first coronal plane with a complete bony transverse lamina, a horizontal plate of bone that separates the olfactory recess from the nasopharyngeal duct (Fig. 1). Measured along the dorsum of the palate, this space is 36.3 mm in rostrocaudal length in *D. leporina*. Maximum height of the nasal cavity is 26.1 mm. Six turbinals are positioned closely adjacent to the nasal septum (Fig. 1). Rostrally, the nasoturbinal and maxilloturbinal are mostly overlapping rostrocaudally. In greatest rostrocaudal length, the nasoturbinal is longer (33.89 mm) than the maxilloturbinal (24.6 mm). To a slight degree, the nasoturbinal overlaps the maxilloturbinal and hides the upper tip of its dorsal lamella in the medial view (Fig. 1). Caudally, four ethmoturbinals are observed (see above regarding some different uses of terminology). The ethmoturbinals are mostly positioned dorsal to the transverse lamina, and are described further below (Fig. 1).

Just above the palate and inferior to the septal cartilage, overlapping the region of the maxillary incisor, the vomeronasal organ resides in the septum (Fig. 2). Rostrally, this organ overlaps with the vomeronasal (paraseptal) cartilages (Figs 2a,b). The vomeronasal cartilage is roughly shaped like an elongated bar, which extends vertically from the sides of the inferior margin of the septal cartilage to a medial position within the osseous vomeronasal capsule; islands or cartilage seen more laterally may be vestiges of more lateral parts of the vomeronasal cartilage (Fig. 2d). It contributes little to support of the vomeronasal organ, however, since the osseous capsule is fully formed by the vomer bone (Figs 2a-c). Some small islands of cartilage are also distributed dorsolaterally within the bony capsule (Fig. 2d). The capsule contains the tubular epithelial vomeronasal organ, nerve bundles, and numerous venous sinuses; the latter are situated medially and ventrally to the vomeronasal organ (Fig. 2d). The vomeronasal neuroepithelium ranges broadly from 40 to 80 μ m in thickness, while the more lateral receptor-free epithelium is typically $\sim 10~\mu$ m thick. The structure of the neuroepithelium is obscured by dense staining with trichrome or hematoxylin-eosin stains; there is a notable lack of cytoplasmic volume (we might speculate this is an artifactual change, perhaps due to incomplete fixation of deeply residing

tissue) in supporting cells and receptor nuclei are only lightly staining and tightly packed (Fig. 2f, inset).

Rostrally, the nasoturbinal and the maxilloturbinal together span the entire height of the nasal fossa (Figs 1, 3a-c, f, g). Each is lined by a highly vascular lamina propria (Figs 3j, k). The maxilloturbinal exhibits grooves on its medial surface which correspond to the position of venous sinuses (Fig. 3k). The nasoturbinal articulates with the nasal bone rostrally (Fig. 3b), but caudally it articulates with the ethmoid, specifically the semicircular lamina; at this caudal level, the nasoturbinal mucosa becomes less vascular (Fig. 3h).

Both the maxilloturbinal and nasoturbinal (Fig. 31) are mostly lined with respiratory epithelium (pseudostratified columnar or similar cuboidal/columnar, ciliated); the side of the maxilloturbinal facing the meatus is lined with a thin transitional epithelium. The nasoturbinal is lacking in any olfactory mucosa, even caudally where it merges with the semicircular lamina; the septum adjacent to it is also non-olfactory at this level (Fig. 31). Most rostrally, the medial side of the semicircular lamina forms the medial wall of the anterolateral recess (Fig. 3h). Within the recess is a thin ciliated epithelial lining (Fig. 3m). More caudally, the semicircular lamina is the medial wall of the frontal recess and bears olfactory epithelium (see below). Of the ethmoturbinals, only ethmoturbinal I projects rostral to the olfactory recess, and in the histologically section this portion of the turbinal is covered by respiratory epithelium.

Recesses of the nasal cavity

There are four recesses that communicate with the main nasal chamber. Three of these constitute a continuous paranasal space. Rostrally, there is a greatly inflated space medial to the semicircular lamina, the anterolateral recess (Fig 4). This recess is rostral to the "lateral root" of the first ethmoturbinal, more formally called the horizontal lamina (Table 1).

At the first coronal plane where the horizontal lamina appears, this plate subdivides the paranasal space into two parts. The horizontal lamina is rather obliquely positioned in the coronal plane (Fig. 5; for a broader context and extended slice series, see suppl. Fig. 1). Dorsomedial to it is the frontal recess, in which there are five turbinals. Four of these project far enough medially to become adjacent to the semicircular lamina (rostrally; Figs 4, 5, 6a, b) or the cribriform plate (caudally; Fig. 5). Both species of *Dasyprocta* have a similar arrangement of frontoturbinals. The spatial relationship is easiest to describe in successive coronal planes (Fig. 5). The first 3 frontoturbinals appear most rostrally, from Dorsomedial (FT1 to lateral (FT3). A fourth FT is restricted more caudally, ventromedial to FT3 (Fig. 5, slice 1343). Finally, another turbinal found caudally is sequestered between FT2 and FT3. This particular turbinal might be termed an interturbinal, because it does not project to a position parallel with the surface of the other FTs (Fig. 5, slice 1478). However, since we have only two specimens to describe, and no developmental information on the developmental timing of formation, this should be considered

a provisional identification. Like the ethmoturbinals, all FTs become more complex caudally. Rostrally, each FT is a simple scroll. FT1 articulates with the nasal bone and scrolls dorsally. FT2 and FT3 arise from the horizontal lamella and scroll dorsally and ventrally, respectively (Fig. 5). Gradually, a second lamella emerges from the opposing side of each FT such that, within the midlevel of the frontal recess, each FT has two secondary lamellae. These lamellae become increasingly scrolled caudally. Most caudally, FT 2-4 extend one lamella medially to contact the cribriform plate (Fig. 5). The cribriform plate is shaped, in cross-section, like the hull of a row-boat (albeit with numerous leaks in the form of olfactory foramina), with the upright sides associating with the frontal recess, while the floor is positioned over the olfactory recess (Fig. 5, slice 1478).

In the histologically sectioned *D. cristata*, the rostral part of most frontoturbinals is covered with non-olfactory epithelium, but the tissue integrity on the frontoturbinals is in moderate or poor condition compared to that in the main chamber and olfactory recess confounding some tissue identification. Epithelium is best preserved in the two turbinals that project most rostrally (FT 2 and 3; Fig. 6c). The most rostral 2.5 mm or 1.8 mm of FTs 2 and 3, respectively, is lined with pseudostratified or simple columnar epithelium, bearing cilia (Fig. 6e). The adjacent surface of the semicircular lamina is covered with pseudostratified columnar ciliated epithelium (Fig 6d). Frontoturbinal 1 and 4 have some olfactory epithelium (Table 2), but the rostral-most sections have poor tissue integrity or poor preservation and therefore it is unclear how much non-olfactory epithelium is present rostrally. On all frontoturbinals, olfactory epithelium appears first in a small patch on the side facing the semicircular lamina; more caudally, the epithelium and lamina propria progressively thickens (Fig. 6f). The epithelium around the interturbinal is absent (poor preservation), making it unclear whether olfactory epithelium is present (Table 2).

The olfactory recess houses most of the ethmoturbinals. Using the rostrocaudal length of the transverse lamina as a proxy, the recess is 22.2 mm long. Maximum height of the olfactory recess is 16.9 mm. All of the ethmoturbinals except the rostral part of ethmoturbinal are I fully housed within the olfactory recess. In the histologically sectioned *D. cristata*, ethmoturbinal I projects rostral to the olfactory recess by approximately 0.5 mm, using the first coronal section in which the space is completely enclosed as the start of the olfactory recess. The CT scan series of *D. leporina* has a more projecting first ethmoturbinal; it projects 5.29 mm rostral to the first CT slice in which the transverse lamina encloses the olfactory recess (right side measurement). Mucosal contours are also visible. The first slice in which mucosa of the first ethmoturbinals is discernable is 5.5 mm rostral to the first slice in which mucosa encloses the olfactory recess. An interturbinal is observed between ethmoturbinals II and III. All ethmoturbinals and the interturbinal possess a simple, folded or plate-like cross-sectional shape rostrally (e.g., Fig. 5, 7b). More caudally, each of them possesses two secondary lamellae (double scrolled; see Fig. 5, slices 1448-1478).

In the histologically sectioned *D. cristata*, ethmoturbinal I bears no olfactory epithelium for the most rostral 1.3 mm (Table 2). Moving caudally, small patches of olfactory epithelium are seen

on lateral and medial sides (but not the dorsal apex) of ethmoturbinal I. No portion of the first ethmoturbinals bearing olfactory epithelium projects rostral to the olfactory recess, although some shrinkage of the rostral part of ethmoturbinals may be assumed (see discussion). The most rostral extent of olfactory epithelium is found along the medial side of the semicircular lamina; this projects rostral to the olfactory recess, and is limited to the semicircular lamina (i.e., it does not extend dorsally to the roof of the nasal cavity at this rostral level). In Figure 4a, the location of this epithelium is estimated by matching the cross-sectional bony contours of ethmoturbinal I in the histologically sectioned *D. cristata*, with the contours of the same bone in CT slices of *D. leporina*. Based on this reconstructed epithelial distribution, most of the space rostral to the olfactory recess is bounded by non-olfactory epithelium (Figs 3, 7).

Olfactory epithelium is observed more rostrally on the semicircular lamina than on the adjacent nasal septum. More caudally where the dorsal edge of the first ethmoturbinals bear olfactory epithelium, both the septal and lateral wall (semicircular lamina) of the main chamber are likewise observed to bear olfactory epithelium (Fig. 7). Here, the entire mucosa thickens due to olfactory nerves and Bowman's glands within the lamina propria, and multiple rows of olfactory sensory neurons within the epithelium, which is approximately 40 µm thick (Figs 7c-e). In the remainder of the olfactory recess, all ethmoturbinals are primarily lined with olfactory epithelium (Table 2). However, numerous artefactual distortions of more caudal ethmoturbinals prevented three reconstructions.

Discussion

The present study provides the most detailed study to date of osteology and histology of a dasyproctid rodent. Dasyproctids are one of many relatively large-bodied New World hystricognaths, and therefore we are able to offer a preliminary assessment of nasal morphology that may vary in relation to body size. Previously, few studies have examined the largest South American hystricognaths (e.g., agoutis, pacaranas, and capybara), aside from studies of the vomeronasal organ (Torres et al., 2020), paranasal sinuses (Ferreira et al., 2022), and the rostral nasal cartilages (Mess, 1999). These studies focused on smaller samples by targeting neonatal and prenatal samples respectively, thus avoiding the difficulties of serially sectioning large specimens. By using μ CT and histology, we are able to present highly detailed nasal anatomy and microanatomy of agoutis for the first time.

Anatomy of the nasal cavity in rodents

Previous detailed work on anatomy of the internal nasal skeleton of rodents has primarily focused on laboratory rodents (e.g., Kelemen, 1950; Harkema et al., 2006; 2012). Monographic works such as that by Dieulafé (1906) and Negus (1958) offer surprising little detail on rodents. Most osteological studies on hystricognath rodents provide only cursory descriptions of the nasal region, if any (e.g., Moreto et al., 2017; Pereira et al., 2019; Rosenfield et al., 2020). A few authors have provided detailed comments on the nasal cavity, or structures therein, of guinea pigs (Dieulafé, 1906; Kelemen, 1950) and chinchillas (Jurcisek et al., 2003), as described in the next section.

In describing rodents (based on rat and guinea pig), Dieulafé (1906) is more detailed than Negus (1958). He describes the maxilloturbinal as having only one upwardly directed "roll." He describes the nasoturbinal in *Cavia* as a lamina (with no scrolling) which descends to partially cover the superior border of the maxilloturbinal. In *Rattus*, Dieulafé describes the nasoturbinal to be rostrocaudally less extensive than the maxilloturbinal. Dieulafé numbers three ethmoturbinals in *Cavia* and four in *Rattus*. However, Kelemen (1950) clearly identifies four ethmoturbinals in *Cavia*. This agrees with our findings on *Dasyprocta*. Furthermore, this is the most common state among non-haplorhine primates (Kollmann and Papin, 1925; Smith and Rossie, 2008), scandentians, dermopterans, (Lundeen and Kirk, 2019), and lagomorphs (Negus, 1958). Thus, this may be plesiomorphic for the superorder Euarchontoglires. Pteropid bats also exhibit this number of ethmoturbinals (Giannini et al., 2012; Smith et al., 2021b). Deviations from this number and most frequently expressed as a reduction in number (e.g., non-pteropid bats, Bhatnagar and Kallen, 1975; haplorhine primates, Maier and Ruf, 2014; Smith et al., 2014).

Descriptions of more peripheral nasal cavity spaces, as well as the smaller turbinals within them, are typically far less detailed in previous work. An exception is Ruf's (2020) thorough discussion of the prenatal nasal "template" (or cartilaginous nasal capsule) as well as the adult skeletal

anatomy of muroid rodents. Muroids have one to two frontoturbinals, and do not have interturbinals within the frontal recess (Ruf, 2020). They may be reduced to only a single ridge (e.g., *Jaculus*) or fully developed with ventral and dorsal scrolls. Of all muroids described by Ruf (2020), only one species possesses more than two frontoturbinals (three are present in *Abrothrix longipilis*). The number of frontoturbinals in some other mammals varies similarly. Most euarchontans have two or fewer frontoturbinals (Lundeen and Kirk, 2019). Lagomorphs also possess two frontoturbinals, and may have an interturbinal between them (Ruf, 2014). With the caveat that some authors may not distinguish interturbinals from frontoturbinals, it appears likely that two turbinals within the frontal recess is the likely plesiomorphic condition in Euarchontoglires. It is the most common condition known among living lagomorphs, scandentians, dermopterans, rodents, and strepsirrhine primates. Exceptions among primates include *Daubentonia madagascarensis*, which has six turbinals in the frontal recess (Maier and Ruf, 2014; Lundeen and Kirk, 2019) and haplorhine primates, which possess none (Lundeen and Kirk, 2019). The most derived exceptions among rodents may be hystricognath rodents (see below).

More broadly in mammals, the plesiomorphic number of frontoturbinals is uncertain, in part due to use of terminology that obscures homology (i.e., "ectoturbinals;" see above). At present, it appears likely that carnivorans and ungulates have the most numerous frontoturbinals, although with much variation. This is also true cumulatively regarding all smaller turbinals. Moore (1981) tabulated a range of 12 to 30 "ectoturbinals" in perissodactyls, and 13 to 20 in artiodactyls.

Numerous studies have stated the presence of maxillary and frontal paranasal spaces, termed recesses (e.g., Adam, 1972; Ruf, 2020) or sinuses in mammals, including rodents (e.g., Harkema et al., 2012; Chamanza and Wright, 2018; Alvites et al., 2018). Previously, some authors have argued that the distinction of a recess and sinus is more than semantic, and hinges on the process of "secondary pneumatization." In secondary pneumatization, opportunistic osteoclastic activity causes a paranasal recess to expand and invade parts of a growing bone (Witmer, 1999; Smith et al., 2005; Rossie, 2006). Thus, if a paranasal space does not opportunistically expand, it is best termed a recess, whereas it is termed a sinus after secondary pneumatization (Rossie, 2006). The extent of secondary pneumatization in rodents has not been subject to serious investigation to our knowledge. However, both the maxillary recess, and the anterolateral recess extending rostral to it, are small spaces in muroid rodents (Adams, 1972; Chamanza and Wright). Some developmental work suggests they may remain small and restricted in both fetuses and adults (Ruf, 2020). Therefore, they may not undergo secondary pneumatization in muroid rodents, in contrast to the invasive expansion seen in the maxillary sinus and some other paranasal spaces in primates (Smith et al., 2005; Rossie, 2006). A comparison to hystricognath rodents is discussed below.

In addition to the descriptions of *Cavia* by Kelemen (1950), Paulli (1900) described nasal anatomy in four of the largest hystricognaths, including *Cuniculus (Coelogenys) paca, Hystrix cristata, Hydrochoerus hydrochaerus*, and *Myocastor (Myopotamus) coypu*. Combined with the present description of *Dasyprocta*, we may make some general observations about these rodents.

Among the large turbinals that project close to the midline ("endoturbinals" of Paulli's terminology), the maxilloturbinal is described in the least detail. Paulli (1900) gave less attention to this turbinal than to the ethmoturbinals and the smaller turbinals. But his description indicates that in *Hystrix* it is a dorsally projecting lamina that intervenes between the nasoturbinal and lateral nasal wall (P 516, "...das maxilloturbinale nach hinten eai hohes blatt bildet, das sich zwischen nasoturbinale und lateraler nasenhöhlenwand ..."). This is consistent with the description of the maxilloturbinal of *Cavia* (Kelemen, 1950) and *Dasyprocta* (Fig. 3f). In *Cavia*, the nasoturbinal is large and rivals the maxilloturbinal in its size having similar rostrocaudal length based on fig. 2 in Kelemen (1950). In *Dasyprocta*, the maxilloturbinal and nasoturbinal together span nearly the entire height of the main nasal chamber (Fig. 1). Qualitatively, these two hystricognaths have quite large nasoturbinals and maxilloturbinals compared to prior descriptions of muroid rodents (e.g., Adams, 1972; Ruf, 2020). Further comparative work to quantify surface areas of these turbinals is needed to confirm this.

Of the more caudal turbinals, nearly all hystricognath rodents studied in detail have four ethmoturbinals, with the notable exception of *Hystrix cristata*, which has an additional ethmoturbinal caudally (Fig. 8A). Smaller turbinals of the ethmoid bone are much more variable in number. Fortunately, Paulli (1900) provides a precise account of their position in several hystricognaths, making it possible to differentiate among the so-called "ectoturbinals." Like many rodents, *Hystrix* possesses two frontoturbinals, and possesses an impressive four interturbinals in the olfactory recess (Fig. 8A). In *Myocastor*, there is only one frontoturbinal indicated by Paulli (1900), and in some species there are none, a possible correlate of semiaquatic behavior (Martinez et al., 2020); no interturbinals in the olfactory recess were have been described in *Myocastor*. In *Hydrochoerus*, there is one frontoturbinal and one interturbinal in the olfactory recess (Fig. 8B). In *Cuniculus (Coelogenys) paca*, Paulli (1900) describes four frontoturbinals and one interturbinal in the olfactory recess. *Dasyprocta*, therefore has the most turbinals in the frontal recess (four frontoturbinals, plus one smaller interturbinal).

The variations in turbinal numbers do not follow a detectable pattern at present. Too few species have been studied to infer phylogenetic patterns, if that is a major factor influencing turbinal numbers. Since *Hydrochoerus* has relatively few ethmoidal turbinals (i.e., all ethmoturbinals, frontoturbinals, interturbinals and nasoturbinal) compared to most hystricognaths that have been studied, it seems the number of smaller turbinals is not under an influence of positive allometry relative to head or body size. Since the smaller turbinals tend to be covered with olfactory epithelium, a correlation to olfactory acuity or discrimination with frontoturbinal and interturbinal numbers could be explored in future studies. Airflow studies suggest that odorants of differing solubility are differentially deposited throughout the nasal fossa (Rygg et al., 2017;

Smith et al., 2019). Thus, the number of turbinals in the frontal versus olfactory recesses may also be of interest. It is possible variation in the different chambers reflects a capacity to detect particular odorants (e.g., based on odorant solubility). Future work could examine this comparatively, taking into account the mucosa type that covers each turbinal (see below).

In addition to varying turbinal numbers, hystricognath rodents vary in the anatomy of recesses in the nasal cavity. All that have been described have a prominent transverse lamina that "captures" most portions of all ethmoturbinals within an olfactory recess. More variation exists in more laterally positioned (paranasal) spaces. Prior descriptions by Paulli (1900) and others (Negus, 1958; Moore, 1981) indicate some paranasal spaces are exceptionally large in hystricognath rodents compared to muroids. However, the identity of specific spaces is complicated by varied terminology. Paulli (1900) describes an enlarged maxillary cavity (Kieferhöhle) in *Myocastor* (Myopotamus) covpu (fig. 29 in Paulli, 1900). Although this space is partially bounded by the maxilla, Paulli's written description (p 516) locates this bone medial to the caudal part of the nasoturbinal ("...medialwarts im hinteren Theil des Nasoturbinale..."). Further, he notes a free margin of the nasoturbinal projects into the space ("...der freie Randtheil des Nasoturbinale, welcher den vorderen Umfang der Öffnung bildet, rollt sich ein wenig in die Höhle ein."). Based on these descriptions, the space is consistent with the anterolateral recess described here. Rather than the nasoturbinal, as defined here, the bone bordering this space is the semicircular lamina (with which the nasoturbinal merges). Its inferior edge in *Dasyprocta* does indeed "roll" upward into the recess; some frontoturbinals project rostrally from the frontal recess into the anterolateral recess (Fig. 6c).

The degree of pneumatic expansion of paranasal spaces also varies, but there clearer examples of "true" sinuses among hystricognaths compared to muroid rodents. Plates from Paulli (1900) reveal that in some of the largest rodents in the world, the inner table of the bone surrounding the frontal recess or parts of the olfactory recess is perforated (Fig. 8); these apertures lead to expanded cavities. Paulli (1900) made reference to "enormous pneumaticity" ("enorme pneumaticitat", p 517) in the skull of *Hystrix cristata* (Fig. 8A), and referred to multiple pneumatic spaces (Fig. 8A). Paulli (1900) also provided a detailed description of two large pneumatic spaces in *Hydrochoerus*. The more rostral space is described to extend into the upper jaw and nasal bone, and then extend caudally and medially to the rear part of the nasoturbinal ("...medialwarts breitet sich die Hohle in ca. hintere Halfte des Naseturbinale ein", p 521). Paulli may be referring to the lamina semicircularis specifically when indicating the rear portion of the nasoturbinal; if so, and based on figure 31 in his monograph (1900), this is consistent with the anterolateral recess. This space is quite inflated in *Hydrochoerus*, similar to *Dasyprocta*. A more caudal pneumatic space invades the frontal bone and extends to the rostral part of the parietal bone. Its ostium connects to the frontal recess, specifically between the nasoturbinal and first frontoturbinal (Fig. 8B). This communication is consistent with the frontal sinus of other mammals (Rossie, 2006).

The extent to which the maxillary or anterolateral recess are pneumatized is unclear, since these spaces do not invade bone by creating perforations (ostia) as described for the frontal or other sinuses described above. The extent to which they pneumatize bone may be made clearer by developmental studies in the future. This information could establish whether the bauplan for these spaces, and the proportions of the facial skeleton, is established early by the cartilaginous template. If so, they may be considered products of primary pneumatization, and could this be called recesses postnatally (Witmer, 1999; Rossie, 2006). Or, these spaces may undergo extensive postnatal changes, perhaps involving secondary pneumatization. In any case, the anterolateral recess appears quite expanded in *Dasyprocta* compared to prior descriptions of muroid rodents (e.g., Adams, 1972, see fig. 1c). Based on the microanatomy of this region (see below), we know this is unrelated to olfactory function, and may be related to scaling of head size.

Functional microanatomy of the nasal cavity in agoutis

Numerous studies have employed cranial skeletal structures as proxies for sensory modalities (e.g., Bhatnagar and Kallen, 1975; Kirk and Kay, 2004; Van Valkenburgh et al., 2004; Green et al., 2012; Muchlinski, 2008; Martinez et al., 2018). The size of skeletal structures such as the cribriform plate has been linked to the repertoire of genes that encode for olfaction (Bird et al., 2018). In cases where skeletal structures have a known functional role, this provides a potentially powerful means to compare functional anatomical element broadly across vertebrate species, or estimate functional capabilities of extinct taxa. For example, the maxilloturbinal bone is lined with a highly vascular respiratory mucosa in a broad array of mammals (Smith et al., 2007; Yee et al., 2016) and the size of this bone has been linked to ecological factors such as climate, which in turn influence demands for conditioning of inspired air (Van Valkenburgh et al., 2011; Green et al., 2012). Many other nasal structures, however, are known to possess more than one type of mucosal covering, i.e., they have dual function (Smith et al., 2007; Yee et al., 2016). This creates a dilemma for drawing inferences based on the size (e.g., cross-sectional area) of bony nasal elements: if turbinals or other structures vary in the proportion of olfactory and non-olfactory mucosal coverings, they may not be easily comparable across taxa.

The extent to which ethmoturbinals are compartmentalized by the transverse lamina varies in mammals such as bats and primates (Eiting et al., 2014). Nonetheless, some mammals have ethmoturbinals that are notably restricted dorsocaudally and mostly sequestered into the olfactory recess by a transverse lamina. In these so-called "macrosmatic" mammals, such canids and rodents, airflow slows within the olfactory recess; this is predicted to maximize odorant uptake (Craven et al., 2009, 2010; Wagner and Ruf, 2021). In this sense, it seems unsurprising that nearly the entirety of ethmoturbinal I, and notably its entire dorsal margin, is lined with olfactory epithelium in *Rattus* and *Peromyscus* (Harkema et al., 2006; Adams, 1972). Still, in both of these rodents a portion of the ethmoturbinals, especially ethmoturbinal I, projects rostral to the olfactory recess (Adams, 1972; Uraih and Maronpot, 1990). In addition, in both of these

rodents, and also in the larger chinchilla (Jurcisek et al., 2003), olfactory epithelium is distributed even further rostrally along the nasoturbinal. Compared to these rodents, *Dasyprocta* has notably less olfactory epithelium distributed rostral to the olfactory recess. Ethmoturbinal I is lined with non-olfactory epithelium for at least the first 1.4 mm (likely an underestimate since free projections of turbinals are known to shrink during histological processing – DeLeon and Smith, 2014). More caudal ethmoturbinals and even the frontoturbinals also possess some non-olfactory epithelium on their most rostral projections. More notable is the complete absence of olfactory epithelium on the nasoturbinal, in contrast to the smaller rodent species from mice to the chinchilla (Adams, 1972; Jurcisek et al., 2003).

Although we could not reliably quantify epithelial surface area on individual turbinals of *Dasyprocta*, in a descriptive sense our findings support the hypothesis that as body size and turbinal size increases in mammals, the proportional extent of olfactory surface area decreases (Smith et al., 2007). To be clear, if the olfactory distribution is *relatively* restricted dorsocaudally in the agouti compared to other rodents, this does not imply relatively diminished olfactory capacity. We have argued elsewhere that olfactory structures should not be expected to scale with body size, and that absolute measurements may be more meaningful than scaled measurements with olfactory (and perhaps other special sensory) structures (Smith and Bhatnagar, 2004). In contrast, nasal surfaces that are dedicated to respiratory function are known to scale closer to isometry (Owerkowicz and Crompton, 2001; Smith et al., 2007). Thus, the apparent "retreat" of olfactory epithelium in the agouti to more caudal regions is likely a reflection of an increased demand for respiratory air-conditioning associated with increasing body size.

If the apparent augmentation of non-olfactory epithelia in *Dasyprocta* and other hystricognaths is borne out quantitatively, an implication is that respiratory mucosa, for filtering, warming and moistening inspired air, may be in great demand in hystricognath rodents based on their generally large body size. This scenario requires further exploration via airflow modeling, as well as a more detailed understanding of the distribution of venous sinuses throughout the mucosal depth of the relatively large rostral turbinals and paranasal spaces of *Dasyprocta* and perhaps other hystricognaths.

Conclusions

The present study offers the most detailed account of the nasal cavity of *Dasyprocta*, or of any large rodent to date, in terms of micro- and gross anatomy. Certain features are notable in this genus compared to other rodents. First, the nasoturbinal is particularly large in dorsoventral and rostrocaudal dimensions in *Dasyprocta*; this turbinal is entirely non-olfactory in function, in apparent contrast to known muroids (Adams, 1972; Harkema, 2006). Whether this relates solely to body size scaling or perhaps also relates to conditioning of inspired air requires more quantitative study. Secondly, olfactory epithelium appears more restricted to the olfactory and

frontal recesses compared to muroids. At the same time, the rostral tips of the olfactory turbinals bear at least some non-olfactory epithelium.

In a broader sense, the findings of this study support the hypothesis that turbinals are multifunctional structures (Smith et al., 2007; Yee et al., 2016), and investigators should use caution when categorizing turbinals as specialized for olfaction. Caution may be especially appropriate in the case of large-bodied mammals, in which the different scaling characteristics of respiratory and olfactory mucosa result in relative more of the former type as body size increases. Further comparative tissue-level studies are sorely needed. Recent advances in the use of μ CT-scanning of iodine-stained samples to identify olfactory tissues may offer an opportunity to identify turbinal mucosa in larger samples of mammals (Yohe et al., 2018; 2021; Smith et al., 2021).

Acknowledgements

We thank Chris Vinyard for CT scanning the specimens used in this study and Hayley Corbin for help with histological staining. Funding, in part, derived from the NSF grants BCS-1830919 and BCS-0959438. We are grateful to Quentin Martinez and one anonymous reviewer, who provided much constructive feedback that greatly improved this report. This report, as much other current work, is written with a deep sense of gratitude to Prof. Kunwar Bhatnagar, who shared many tissue processing techniques with the first author, such as the decalcifying solution used in this study.

References

Adams DR (1972) Olfactory and non-olfactory epithelia in the nasal cavity of the mouse, *Peromyscus*. American Journal of Anatomy 133: 37–50. https://doi.org/10.1002/aja.1001330104

Adams DR, McFarland LZ (1972) Morphology of the nasal fossae and associated structures of the hamster (*Mesocricetus auratus*). Journal of Morphology 137: 161–180. https://doi.org/10.1002/jmor.1051370204

Alvites RD, Caseiro AR, Pedrosa SS, Branquinho ME, Varejao ASP, Mauricio AC (2018) The nasal cavity of the rat and mouse-source of mesenchymal stem cells for treatment of peripheral nerve injury. Anatomical Record 301: 1678–1689. https://doi.org/10.1002/ar.23844

Barrios, A. W., Núñez, G., Sánchez Quinteiro, P., & Salazar, I (2014) Anatomy, histochemistry, and immunohistochemistry of the olfactory subsystems in mice. Frontiers in Neuroanatomy 8: 63. https://doi.org/10.3389/fnana.2014.00063

Bhatnagar KP, Kallen FC (1975) Quantitative observations on the nasal epithelia and olfactory innervation in bats. Acta Anatomica 91: 272–282. https://doi.org/10.1159/000144389

Bird DJ, Murphy WJ, Fox-Rosales L, Hamid I, Eagle RA, Van Valkenburgh B (2018) Olfaction written in bone: cribriform plate size parallels olfactory receptor gene repertoires in Mammalia. Proceedings of the Royal Society B, Biological Sciences 285: 20180100. http://doi.org/10.1098/rspb.2018.0100

Boël M, Romestaing C, Duchamp C, Veyrunes F, Renaud S, Roussel D, Voituron Y (2020) Improved mitochondrial coupling as a response to high mass-specific metabolic rate in extremely small mammals. Journal of Experimental Biology 223: jeb215558. https://doi.org/10.1242/jeb.215558

Chamanza R, Wright JA (2015) A review of the comparative anatomy, histology, physiology and pathology of the nasal cavity of rats, mice, dogs and non-human primates. Relevance to Inhalation Toxicology and Human Health Risk Assessment. Journal of Comparative Pathology 153: 287–314. https://doi.org/10.1016/j.jcpa.2015.08.009

Clancy AN, Schoenfeld TA, Forbes WB, Macrides F (1994) The spatial organization of the peripheral olfactory system of the hamster. Part II: receptor surfaces and odorant passageways within the nasal cavity. Brain Research Bulletin 34: 211–241. https://doi.org/10.1016/0361-9230(94)90060-4

Craven BA, Paterson EG, Settles GS, Lawson MJ (2009) Development and Verification of a High-Fidelity Computational Fluid Dynamics Model of Canine Nasal Airflow. Journal of Biomechanical Engineering 131: 091002. https://doi.org/10.1115/1.3148202

Craven BA, Paterson EG, Settles GS (2010) The fluid dynamics of canine olfaction: unique nasal airflow patterns as an explanation of macrosmia. Journal of the Royal Society Interface 7: 933–943. https://doi.org/10.1098/rsif.2009.0490

DeLeon VB, Smith, TD (2014). Mapping the nasal airways: using histology to enhance CT-based three-dimensional reconstruction in *Nycticebus*. Anatomical Record 297: 2113–2120. https://doi.org/10.1002/ar.23028

D'Elía G, Fabre P H, Lessa EP (2019). Rodent systematics in an age of discovery: recent advances and prospects. Journal of Mammalogy 100: 852–871. https://doi.org/10.1093/jmammal/gyy179

Dieulafé L (1906) Morphology and embryology of the nasal fossae of vertebrates. Annals of Otology Rhinology and Laryngology 15: 1–584. https://doi.org/10.1177/000348940601500214

Eiting T, Smith TD, Dumont ER (2014) Olfactory epithelium in the olfactory recess: a case study in new world leaf-nosed bats. Anatomical Record 297: 2105–2112. https://doi.org/10.1002/ar.23030

Ferreira JD, Dozo MT, Bundué JM, Kerber L (2022) Morphology and postnatal ontogeny of the cranial endocast and paranasal sinuses of capybara (*Hydrochoerus hydrochaeris*), the largest living rodent. Journal of Morphology 283: 66–90. https://doi.org/10.1002/jmor.21428

Gignac PM, Kley NJ (2014) Iodine-enhanced micro-CT imaging: methodological refinements for the study of the soft-tissue anatomy of post-embryonic vertebrates. Journal of Experimental Zoology B, Molecular and Developmental Evolution 322: 166–176. https://doi.org/10.1002/jez.b.22561

Giannini NP, Macrini TE, Wible JR, Rowe TB, Simmons NB (2012) The internal nasal skeleton of the bat *Pteropus lylei* K. Anderson, 1908 (Chiroptera: Pteropodidae). Annals of the Carnegie Museum 81: 1–17.

Green P, Van Valkenburgh B, Pang B, Bird D, Rowe T, Curtis A (2012) Respiratory and olfactory turbinal size in canid and arctoid carnivorans. Journal of Anatomy 221: 609–6021. https://doi.org/10.1111/j.1469-7580.2012.01570.x

Gross EA, Swenberg JA, Fields S, Popp JA (1982) Comparative aspects of the nasal cavity in rats and mice. Journal of Anatomy 135: 83–88.

Gurtovoi NN (1966) Ecological-morphological differences in the structure of the nasal cavity in the representatives on the orders Insectivora, Chiroptera and Rodentia. Zoologischeskii Zhurnal 45: 1536–1551.

Harkema JR, Carey SA, Pestka JJ (2006) The nose revisited: a brief review of the comparative structure, function, and toxicologic pathology of the nasal epithelium. Toxicologic Pathology 34: 252–269. https://doi.org/10.1080/01926230600713475

Harkema JR, Carey SA, Wagner JG, Dintzis SM, Liggitt D (2012) Nose, paranasal sinuses, pharynx, and larynx. In: Piper M, Treuting SM, Dintzis MD (Eds) Comparative Anatomy and Histology: A Mouse and Human Atlas. Elsevier, New York, 71–94.

Ito K, Tu VT, Eiting T P, Nojiri T, Koyabu D (2021). On the Embryonic Development of the Nasal Turbinals and Their Homology in Bats. Frontiers in Cell and Developmental Biology, 9: 379. https://doi.org/10.3389/fcell.2021.613545

Jiang J, Zhao K (2010) Airflow and nanoparticle deposition in rat nose under various breathing and sniffing conditions a computational evaluation of the unsteady effect. Journal of Aerosol Science 41: 1030–1043. https://doi.org/10.1016/j.jaerosci.2010.06.005

Jurcisek JA, Durbin JE, Kusewitt DF, Bakaletz LO (2003) Anatomy of the nasal cavity in the chinchilla. Cells Tissues Organs 174: 136–52. https://doi.org/10.1159/000071154

Kelemen G (1950) Nasal cavity of the guinea pig in experimental work. AMA archives of otolaryngology 52: 579–596. https://doi.org/10.1001/archotol.1950.00700030603006

Kimbell JS, Godo MN, Gross EA, Joyner DR, Richardson RB, Morgan KT (1997) Computer simulation of inspiratory airflow in all regions of the F344 rat nasal passages. Toxicology and Applied Pharmacology 145: 388–398. https://doi.org/10.1006/taap.1997.8206

Kirk EC, Kay RF (2004) The evolution of high visual acuity in the Anthropoidea. In: Ross CF, Kay RF (Eds) Anthropoid Origins: New Visions. Kluwer Academic/Plenum Publishers, New York, 539–602. https://doi.org/10.1007/978-1-4419-8873-7_20

Kollmann M, Papin L (1925) Etudes sur lémuriens. Anatomie compareé des fosses nasales et de leurs annexes. Archives de Morphologie Générale et Expérimentale 22: 1–60.

Larochelle L, Baron G (1989) Comparative morphology and morphometry of the nasal fossae of four species of North American shrews (Soricinae). American Journal of Anatomy 186: 306–314. https://doi.org/10.1002/aja.1001860307

Laska M, Fendt M, Wieser A, Endres T, Hernandez Salazar LT, Apfelbach R (2005) Detecting danger - or just another odorant? Olfactory sensitivity for the fox odor component 2,4,5-trimethylthiazoline in four species of mammals. Physiology & Behavior 84: 211–215. https://doi.org/10.1016/j.physbeh.2004.11.006

Lawson MJ, Craven BA, Paterson EG, Settles GS (2012) A Computational Study of Odorant Transport and Deposition in the Canine Nasal Cavity: Implications for Olfaction. Chemical Senses 37: 553–566. https://doi.org/10.1093/chemse/bjs039

Lee MK, Rebhun LI, Frankfurter A (1990) Posttranslational modification of class III β-tubulin. Proceedings of the National Academy of Sciences 87: 7195–7199. https://doi.org/10.1073/pnas.87.18.7195

Lischka FW, Gomez G, Yee KK, Dankulich-Nagrudny L, Lo L, Haskins ME, Rawson NE (2008) Altered olfactory epithelial structure and function in feline models of mucopholysaccharidoses I and VI. Journal of Comparative Neurology 511: 360–372. https://doi.org/10.1002/cne.21847

Lundeen IK, Kirk EC (2019) Internal nasal morphology of the Eocene primate *Rooneyia viejaensis* and extant Euarchonta: Using μCT scan data to understand and infer patterns of nasal fossa evolution in primates. Journal of Human Evolution 132: 137–173. https://doi.org/10.1016/j.jhevol.2019.04.009

MacDonald DW, Herrera EA, Ferraz KMPMB, Moreira, JB (2012) The capybara paradigm: from sociality to sustainability. In: Moreira JR, Ferraz KMPMB, Herrera EA, Macdonald DW (Eds) Capybara: Biology, Use and Conservation of an Exceptional Neotropical Species. Springer, New York, 385-402

Macrini TE (2014) Development of the ethmoid in *Caluromys philander* (Didelphidae, Marsupialia) with a discussion on the homology of the turbinal elements in marsupials. The Anatomical Record 297: 2007–2017. https://doi.org/10.1002/ar.23024

Maier W, Ruf I (2014) Morphology of the nasal capsule of primates--with special reference to *Daubentonia* and *Homo*. Anatomical Record 297: 2018–2030. https://doi.org/10.1002/ar.23023

Maier W (1993a) Cranial morphology of the therian common ancestor, as suggested by the adaptations of neonate marsupials. In: Szalay FS, Novacek MJ, McKenna MC (Eds) Mammal Phylogeny. Springer, New York, NY, 165–181.

Maier W (1993b) Zur evolutiven und funktionellen Morphologie des Gesichtsschädels der Primaten. Zeitschrift für Morphologie und Anthropologie 79: 279–299. https://doi.org/10.1127/zma/79/1992/279

Maier W (2020) A neglected part of the mammalian skull: The outer nasal cartilages as progressive remnants of the chondrocranium. Vertebrate Zoology 70: 367–382. https://doi.org/10.26049/VZ70-3-2020-09

Maier W, Schrenk F (1987) The hystricomorphy of the Bathyergidae, as determined from ontogenetic evidence. Zeitschrift für Säugtierkunde 52: 156–164.

Martinez Q, Lebrun R, Achmadi AS, Esselstyn JA, Evans AR, Heaney LR, Miguez RP, Rowe KC, Fabre PH (2018) Convergent evolution of an extreme dietary specialisation, the olfactory

system of worm-eating rodents. Scientific reports, 8: 1–13. https://doi.org/10.1038/s41598-018-35827-0

Martinez Q, Clavel J, Esselstyn JA, Achmadi AS, Grohé C, Pirot N, Fabre, PH (2020) Convergent evolution of olfactory and thermoregulatory capacities in small amphibious mammals. Proceedings of the National Academy of Sciences 117: 8958–8965. https://doi.org/10.1073/pnas.1917836117

Mess A (1999) The rostral nasal skeleton of hystrognath rodents: evidence on their phylogenetic relationships. Zoosystematics and Evolution 75: 19–35. https://doi.org/10.1002/mmnz.19990750104

Moore WJ (1981) The Mammalian Skull. Cambridge University Press, Cambridge. 369 p.

Moreto AO, Oliveira FD, Bertassoli BM, Assis Neto AC (2017) Morfologia comparada do aparelho respiratório de capivaras (*Hydrochoerus hydrochoeris*). Morfofisiologia 37: 269–277. https://doi.org/10.1590/S0100-736X2017000300011

Muchlinski MN (2008) The relationship between the infraorbital foramen, infraorbital nerve, and maxillary mechanoreception: implications for interpreting the paleoecology of fossil mammals based on infraorbital foramen size. Anatomical Record 291: 1221–1226. https://doi.org/10.1002/ar.20742

Negus V (1958) The Comparative Anatomy and Physiology of the Nose and Paranasal Sinuses. Livingston, Edinburgh and London. 402 p.

Nomina Anatomica Veterinaria (2005) www.wava-amav.org/nav.htm

Novacek MJ (1993) Patterns of diversity in the mammalian skull. In: Hanken J, Hall BK (Eds) The Skull, vol. 2. Chicago University Press, Chicago, 438–545.

Owerkowicz T, Crompton AW (2001) Allometric scaling of respiratory turbinates and trachea in mammals and birds. Journal of Vertebrate Paleontology 21(Suppl): 86A.

Pang B, Yee KK, Lischka FW, Rawson NE, Haskins ME, Wysocki CJ, Craven BA, Van Valkenburgh B (2016) The influence of nasal flow on respiratory and olfactory epithelial distribution in felids. Journal of Experimental Biology 219: 1866–1874. https://doi.org/10.1242/jeb.131482

Paulli S (1900) Über die Pneumaticität des Schädels bei den Säugethieren. III. Über die Morphologie des Siebbeins der Pneumaticität bei den Insectivoran, Hyracoideen, Chiropteren, Carnivoren, Pinnepedien, Edentates, Rodentiern, Prosimien und Primaten. Gegenbaurs Morphologisches Jahrbuch 28: 483–564.

Pereira FMAM, Bete SBDS, Inamassu LR, Mamprim MJ, Schimming BC (2020) Anatomy of the skull in the capybara (*Hydrochoerus hydrochaeris*) using radiography and 3D computed tomography. Anatomia Histologia Embryologia 49: 317–324. https://doi.org/10.1111/ahe.12531

Ranslow AN, Richter JP, Neuberger T, Van Valkenburgh B, Rumple CR, Quigley AP, Pang B, Krane MH, Craven BA (2014) Reconstruction and morphometric analysis of the nasal airway of the white-tailed deer (*Odocoileus virginianus*) and implications regarding respiratory and olfactory airflow. Anatomical Record 297: 2138–2147. https://doi.org/10.1002/ar.23037

Ribeiro P F, Manger PR, Catania KC, Kaas JH, Herculano-Houzel S (2014) Greater addition of neurons to the olfactory bulb than to the cerebral cortex of eulipotyphlans but not rodents, afrotherians or primates. Frontiers in Neuroanatomy 8: 23. https://doi.org/10.3389/fnana.2014.00023

Robinson JG, Redford KH (1986) Body size, diet, and population density of neotropical mammals. American Naturalist 128: 665–680.

Rosenfield DA, Paretsis NF, Yanai PR, Pizzutto CS (2020) Gross osteology and digital radiography of the common capybara (*Hydrochoerus hydrochaeris*), Carl Linnaeus, 1766 for scientific and clinical application. Brazilian Journal of Veterinary Research and Animal Science 57: e172323. https://doi.org/10.11606/issn.1678-4456.bjvras.2020.172323

Rouquier S, Blancher A, Giorgi D (2000) The olfactory receptor gene repertoire in primates and mouse: Evidence for reduction of the functional fraction in primates. Proceedings of the National Academy of Sciences 97: 2870–2874. https://doi.org/10.1073/pnas.040580197

Rossie JB (2006) Ontogeny and homology of the paranasal sinuses in Platyrrhini (Mammalia: Primates). Journal of Morphology 267: 1–40. https://doi.org/10.1002/jmor.10263

Ruf I (2014) Comparative anatomy and systematic implications of the turbinal skeleton in Lagomorpha (Mammalia). The Anatomical Record 297: 2031–2046. https://doi.org/10.1002/ar.23027

Ruf I, Maier W, Rodrigues PG, Schultz CL (2014) Nasal anatomy of the non-mammaliaform cynodont *Brasilitherium riograndensis* (Eucynodontia, Therapsida) reveals new insight into mammalian evolution. Anatomical Record 297: 2018–2030. https://doi.org/10.1002/ar.23022

Ruf I (2020) Ontogenetic transformations of the ethmoidal region in Muroidea (Rodentia, Mammalia): new insights from perinatal stages. Vertebrate Zoology 70: 383–415. https://doi.org/10.26049/VZ70-3-2020-10

Rygg AD, Van Valkenburgh B, Craven BA (2017) The influence of sniffing on airflow and odorant deposition in the canine nasal cavity. Chemical Senses 42: 683–698. https://doi.org/10.1093/chemse/bjx053 Schreider JP, Raabe OG (1981) Anatomy of the nasal-pharyngeal airway of experimental animals. Anatomical Record 200: 195–205. https://doi.org/10.1002/ar.1092000208

Smith TD, Bhatnagar KP (2004) "Microsmatic" primates: Reconsidering how and when size matters. Anatomical Record 279B: 24–31. https://doi.org/10.1002/ar.b.20026

Smith TD, Bhatnagar KP, Rossie JB, Docherty BA, Burrows AM, Cooper GM, Mooney MP, Siegel MI (2007) Scaling of the first ethmoturbinal in nocturnal strepsirrhines; olfactory and respiratory surfaces. Anatomical Record 290: 215–237. https://doi.org/10.1002/ar.20428

Smith TD, Craven BA, Engel SM, Bonar CJ, DeLeon VB (2019) Nasal airflow in the pygmy slow loris (*Nycticebus pygmaeus*) based on a combined histological, computed tomographic and computational fluid dynamics methodology. Journal of Experimental Biology 222 (Pt 23): jeb207605. https://doi.org/10.1242/jeb.207605

Smith TD, Craven BA, Engel SM, Van Valkenburgh B, DeLeon VB (2021) "Mucosal maps" of the canine nasal cavity: micro-computed tomography and histology. Anatomical Record 304: 127–138. https://doi.org/10.1002/ar.24511

Smith TD, Eiting TP, Bonar CJ, Craven BA (2014) Nasal morphometry in marmosets: loss and redistribution of olfactory surface area. Anatomical Record 294: 2093–2014. https://doi.org/10.1002/ar.23029

Smith TD, Rossie, JB (2008) The nasal fossa of mouse and dwarf lemurs (Primates, Cheirogaleidae). Anatomical Record 291:895–915. https://doi.org/10.1002/ar.20724

Smith TD, Rossie JB, Cooper GM, Mooney MP, Siegel MI (2005) Secondary pneumatization in the maxillary sinus of callitrichid primates: insights from immunohistochemistry and bone cell distribution. Anatomical Record 285: 677–689. https://doi.org/10.1002/ar.a.20209

Smith TD, Siegel MI, Bhatnagar KP (2001) Reappraisal of the vomeronasal system of catarrhine primates, ontogeny, morphology, functionality, and persisting questions. Anatomical Record 265B:176–192. https://doi.org/10.1002/ar.1152

Starck D (1975) The development of the chondrocranium in primates. In: Luckett WP, Szalay FS (Eds) Phylogeny of the Primates. Plenum, New York, 127–155.

Torres MV, Ortiz-Leal I, Villamayor PR, Ferreiro A, Rois JR, Sanchez-Quinteiro P. (2020) The vomeronasal system of the newborn capybara: a morphological and immunohistochemical study. Scientific Reports 10: 13304. https://doi.org/10.1038/s41598-020-69994-w

Uraih LC, Maronpot RR (1990) Normal histology of the nasal cavity and application of special techniques. Environmental Health Perspectives 85: 187–208. https://doi.org/10.1289/ehp.85-1568325

Van Valkenburgh B, Theodor J, Friscia A, Pollack A, Rowe T (2004) Respiratory turbinates of canids and felids: a quantitative comparison. Journal of Zoology, London 264: 281–293. https://doi.org/10.1017/S0952836904005771

Van Valkenburgh B, Curtis A, Samuels JX, Bird D, Fulkerson B, Meachen-Samuels J, Slater G. (2011) Aquatic adaptations in the nose of carnivorans: Evidence from the turbinates. Journal Anatomy 218: 298–310. https://doi.org/10.1111/j.1469-7580.2010.01329.x

Van Valkenburgh B, Pang B, Bird D, Curtis AC, Yee K, Wysocki C, Craven BA (2014a) Anatomical Record 297: 2065–2097. https://doi.org/10.1002/ar.23026

Van Valkenburgh B, Smith TD Craven BA. (2014b) Tour of a labyrinth: exploring the vertebrate nose. Anatomical Record, 297: 1975–1984. https://doi.org/10.1002/ar.23021

Vander Wall SB, Beck MJ, Briggs JS, Roth JK, Thayer TC, Hollander JL, Armstrong JM (2003) Interspecific variation in the olfactory abilities of granivorous rodents. Journal of Mammalogy 84: 487–496. https://doi.org/10.1644/1545-1542(2003)084<0487:IVITOA>2.0.CO;2

Wagner F, Ruf I (2021) 'Forever young' – Postnatal growth inhibition of the turbinal skeleton in brachycephanic dog breeds (*Canis lupus familiaris*, Canidae, Carnivora). Anatomical Record 304:154–189. https://doi.org/10.1002/ar.24422

Wang R-G, Jiang S-C, Gu R (1994) The cartilaginous nasal capsule and embryonic development of human paranasal sinuses. Journal of Otolaryngology 23: 239–243.

Weiler E, Apfelbach R, Farbman AI (1999) The vomeronasal organ of the male ferret. Chemical Senses 24: 127–136. https://doi.org/10.1093/chemse/24.2.127

Wible JR (2011) On the treeshrew skull (Mammalia, Placentalia, Scandentia). Annals of the Carnegie Museum 79: 149–230. https://doi.org/10.2992/007.079.0301

Witmer LM (1999) The phylogenetic history of the paranasal air sinuses. In: Koppe T, Nagai H, Alt KW (Eds) The Paranasal Sinuses of Higher Primates. Quintessence, Berlin, 21–34.

Yee KK, Craven BA, Wysocki C J, Van Valkenburgh B (2016) Comparative morphology and histology of the nasal fossa in four mammals: gray squirrel, bobcat, coyote, and white-tailed deer. Anatomical Record 299: 840–852. https://doi.org/10.1002/ar.23352

Yohe LR, Hoffmann S, Curtis A (2018) Vomeronasal and olfactory structures in bats revealed by DiceCT clarify genetic evidence of function. Frontiers in Neuroanatomy 12: 32. https://doi.org/10.3389/fnana.2018.00032

Yohe LR, Fabbri M, Lee D, Davies K, Yohe TP, Sánchez KR, Rengifo EM, Hall R, Mutumi G, Hedrick BP, Sadier A, Simmons NB, Sears KE, Dumont E, Rossiter SJ, Bullar B-A, Dávalos,

LM (2021) Ecological constraints on highly evolvable olfactory receptor genes and morphology. bioRxiv. https://doi.org/10.1101/2021.09.06.459178

Zhao K, Dalton P, Yang GC, Scherer PW (2006) Numerical modeling of turbulent and laminar airflow and odorant transport during sniffing in the human and rat nose. Chemical Senses 31: 107–118. https://doi.org/10.1093/chemse/bjj008

Figure captions

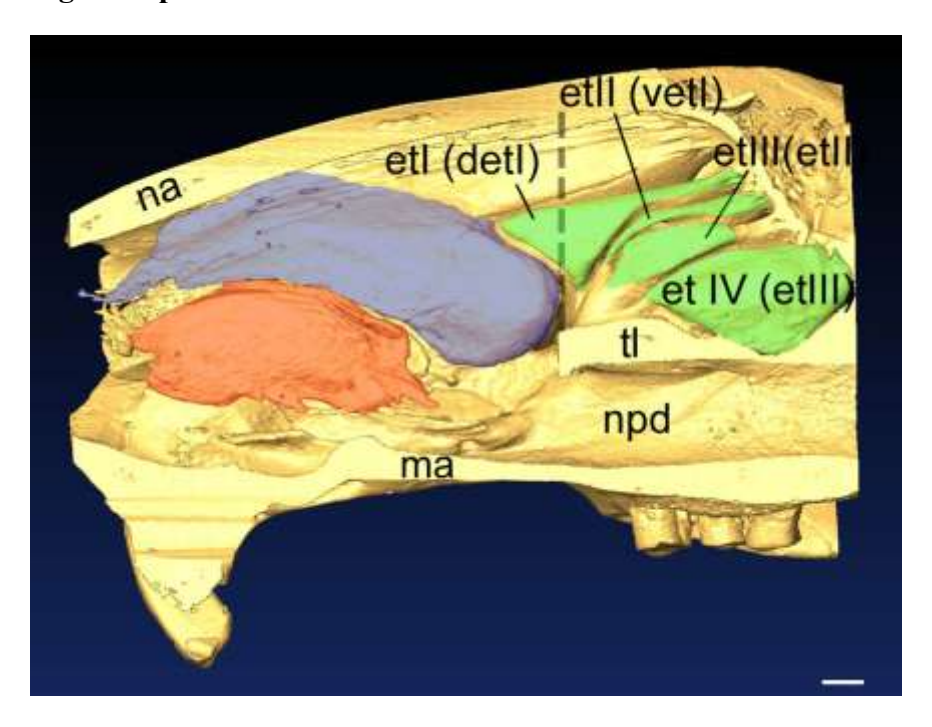


Figure 1. View of the lateral wall of the right nasal fossa in an adult agouti (*Dasyprocta leporina*), with the largest turbinals color-coded as light red (maxilloturbinal), purple (nasoturbinal) and green (ethmoturbinals). Most of the ethmoturbinals are within the olfactory recess (the space to the right side of the dashed line), which is found dorsal to the transverse lamina (tl). et I, et II, et III, et IV, first through fourth ethmoturbinals (in parentheses, synonyms from other recent studies are included, see Table 1); ma, maxillary bone; na, nasal bone; npd, nasopharyngeal duct. Scale bar: 3 mm.

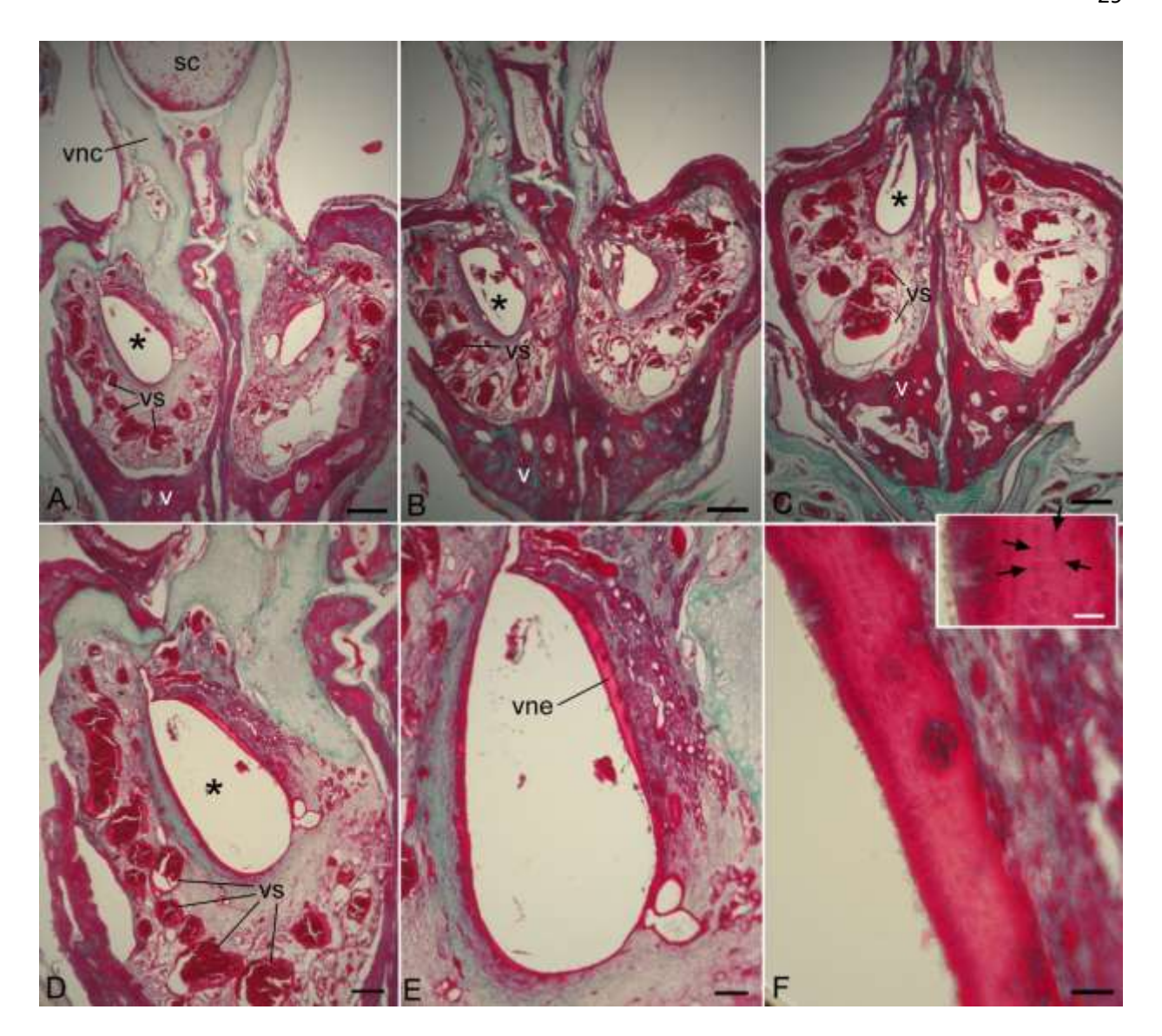


Figure 2. Coronal sections of the vomeronasal organ of adult agouti (*Dasyprocta cristata*), shown at levels A) within the rostral half; B) the approximate midpoint, and C) near the caudalmost limit of vomeronasal neuroepithelium (vne; * = lumen). D-F and inset, increasing magnifications of A. The inset of F reveals faintly stained rows of nuclei (arrows) in the vne. Gomori trichrome stain (bone, stained red or green; cartilage, light green; vne is atypically stained red in this specimen). sc, septal cartilage; vnc, vomeronasal cartilage; vs, venous sinuses. v, vomer. Scale bars: A-C, 0.5 mm; D, 200 μm; E, 100 μm; F, 20 μm, inset, 10 μm.

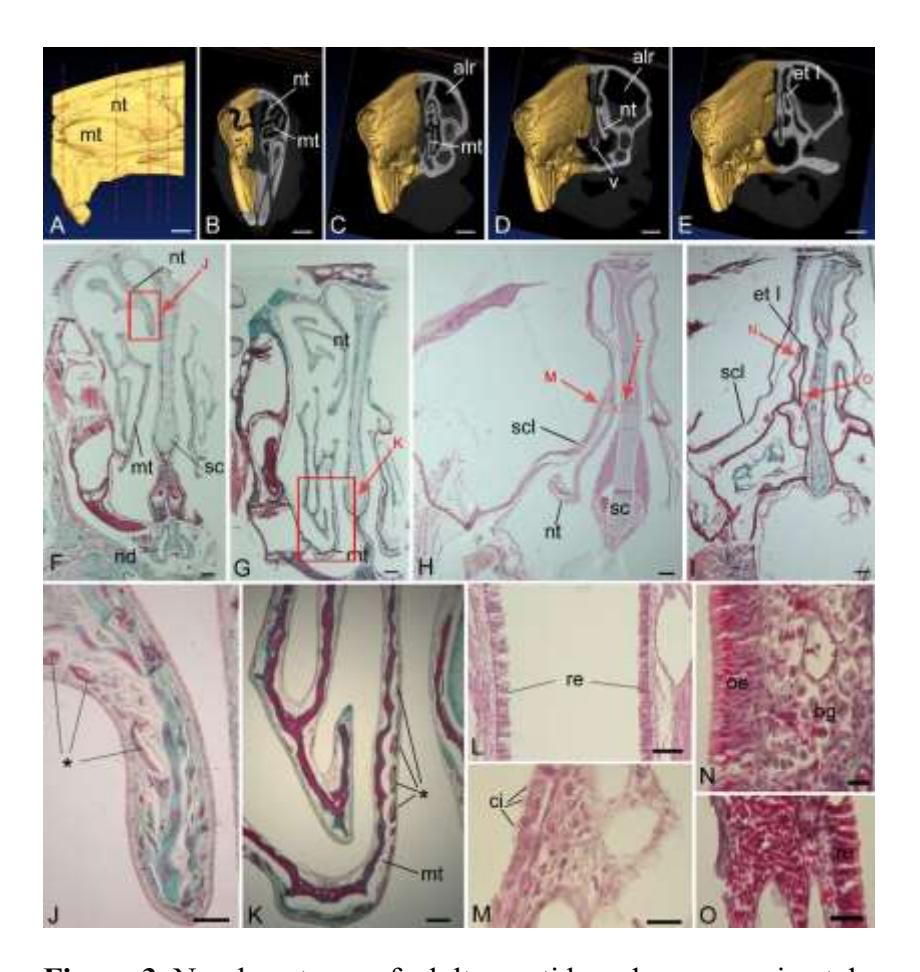


Figure 3. Nasal anatomy of adult agouti based on approximately matching levels of μm-CT slices of Dasyprocta leporina and histological sections of Dasyprocta cristata. A) Threedimensional reconstruction of the part of the nasal fossa from rostral opening to the start of the olfactory recess, with coronal cross-sections indicated by dashed lines that represent, from rostral to caudal, plates B-E. Plates B to E are matched to sections showing the same features from a different specimen in plates F to I. The most rostral level (B, F) includes the rostral extent of the maxilloturbinal (mt) and nasoturbinal (nt), as well as the nasopalatine, or incisive duct (nd). Closer to the midpoint of these turbinals, each becomes more complex by virtue of additional lamellae. Enlarged views of both the nt (J) and mt (K) reveal numerous venous sinuses (*) within the lamina propria (boxes in f and g indicate source of enlarged views). From cross-sectional levels C to E, a paranasal recess is found lateral to the nasal fossa (alr = anterolateral recess). The ALR becomes quite large by sectional level d, and the nasal fossa is thus narrowed. Also at this level, the NT merges with the semicircular lamina (H, scl). 1) The adjacent surfaces of the nt and septum are lined by respiratory epithelium (re) at the level shown in H; the alr is lined by ciliated (ci) simple cuboidal epithelium. Cross-sectional level E/I reveals ethmoturbinal I (etI) at the start of the olfactory recess. Here, the lateral and medial sides of the dorsal part of etI (enlarged in N) is lined with olfactory epithelium (oe), while more ventrally et I is lined with re (enlarged in O). Stains F, G, I, J, K, N, O: Gomori trichrome; H, L, M: hematoxylin-eosin. sc, septal cartilage. Scale bars: A-E, 5 mm; F-I, 1 mm; J, 30 μm; K, 400 μm; L, 50 μm; M-O, 20 μm.

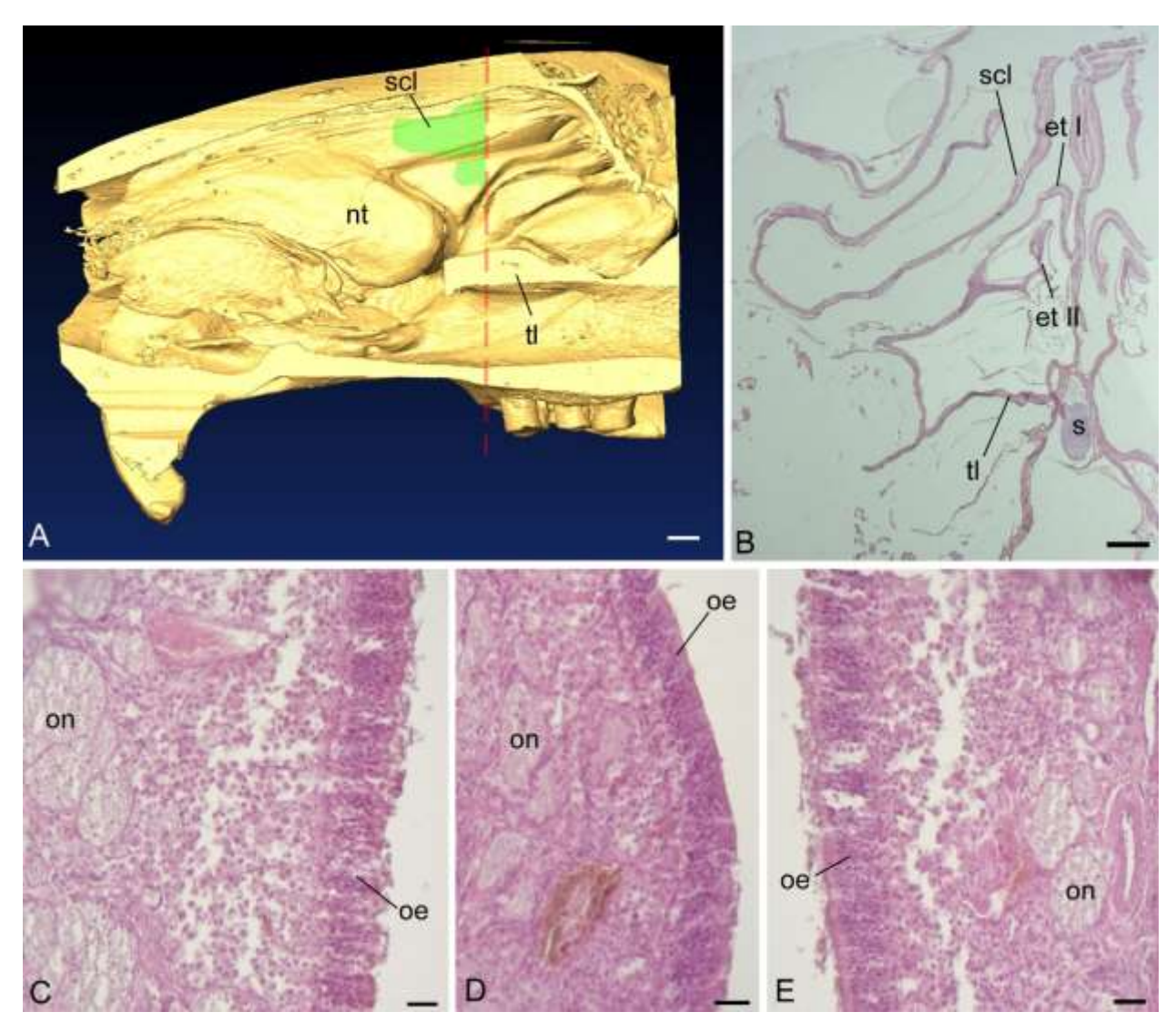


Figure 4. Left frontal recess of an adult *Dasyprocta cristata*, seen from the medial side after the ethmoturbinal complex and the semicircular lamina are entirely removed. The dorsal root of the semicircular lamina (sl) is indicated, as is the ventral connection of the horizontal lamina (hl). Three frontoturbinals (ft) are visible adjacent to the lateral part of the cribriform plate (cp). alr, anterolateral recess. Scale bar: 2.5 mm.

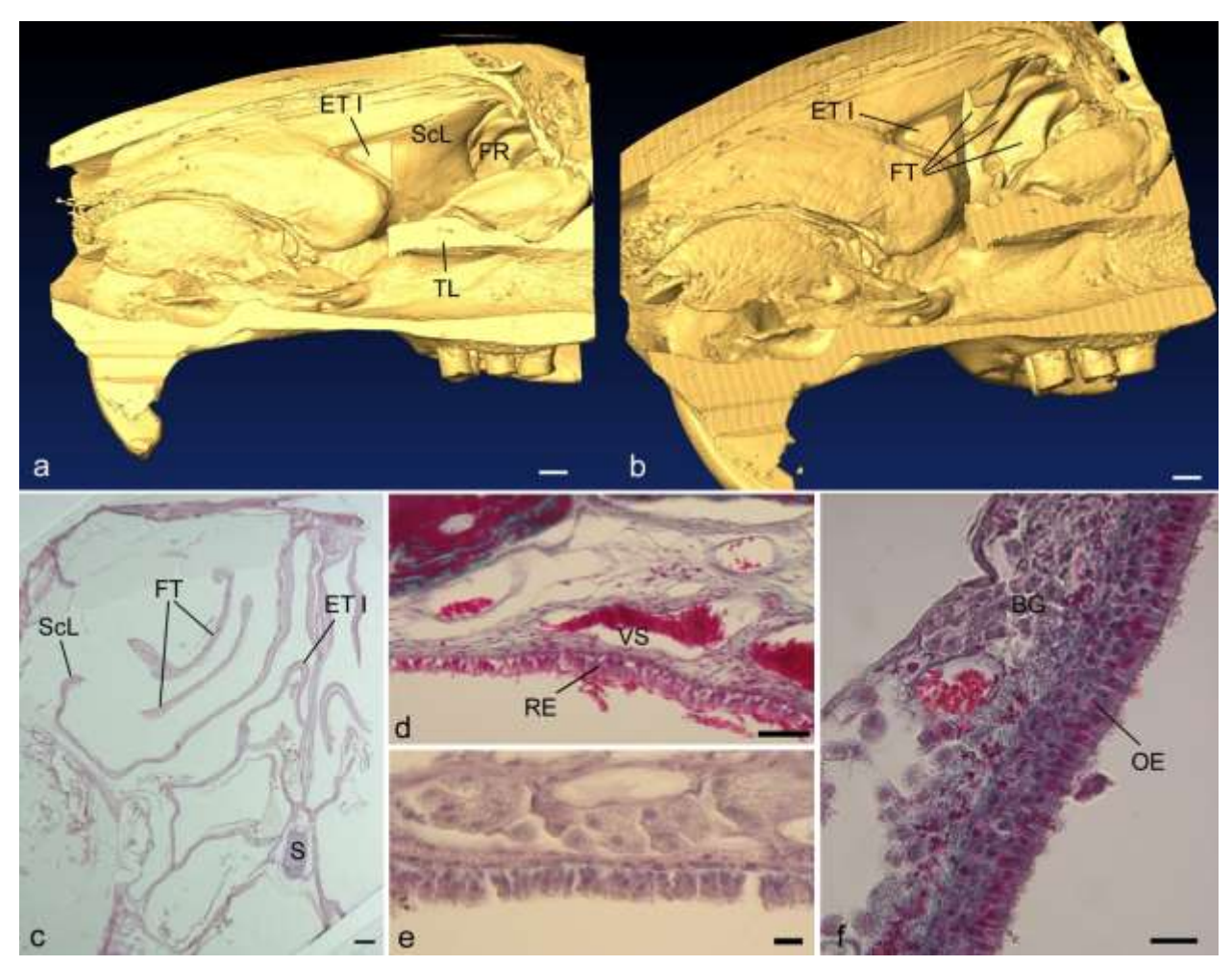


Figure 5. Rostral to caudal CT slices of *Dasyprocta leporina*, spanning the space of the frontal recess (numbers indicate rostrocaudal CT slice level). The semicircular lamina is tinted red; frontoturbinals are tinted green. Slice 1278 is near the rostral ends of the first three frontoturbinals (ft1-3), at a position where the semicircular lamina (sl) would obscure view of these turbinals from the medial side. Note the horizontal lamina (hl) is a ventral attachment for ft2 and ft3. At slice 1278, note the frontal recess (fr) is the space dorsal to the hl, and a very compressed maxillary recess (mr) is positioned ventrolateral to the hl. At slice 1343, a fourth frontoturbinal (ft4) has emerged, and this turbinal gradually projects parallel to F1-3 at more caudal levels. At slice 1478, the emergence of an interturbinal (it) between ft2 and ft3 is visible. All frontoturbinals become double-scrolled caudally; the more ventromedial lamella ultimately fused with the cribriform plate (cp). or, olfactory recess. Scale bar: 3 mm.

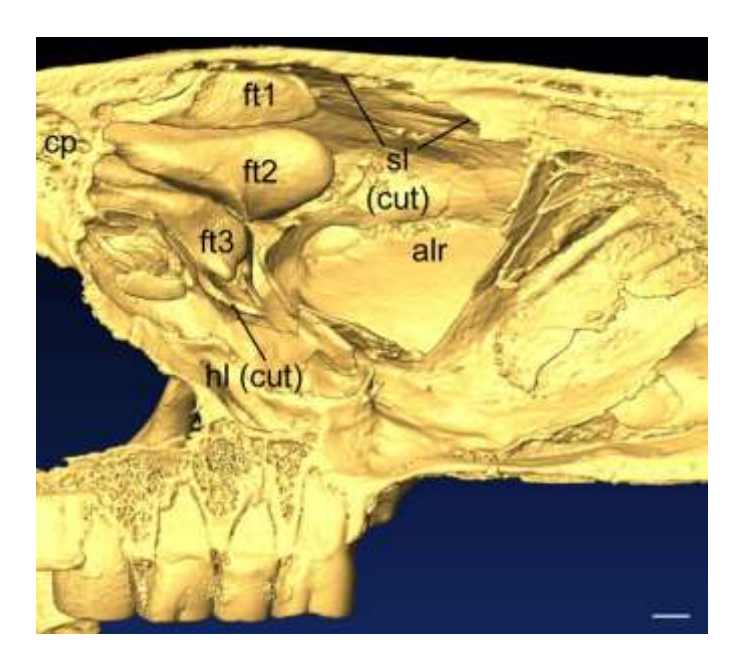


Figure 6. A), B), medial and rostromedial perspectives of the right nasal fossa in an adult agouti (*Dasyprocta leporina*). In A, the caudal part of the first ethmoturbinal (etl), the entire second and third ethmoturbinals, as well as their root lamella are virtually dissected away to reveal the semicircular lamina (scl). Caudal to the scl is the opening into the frontal recess (fr). In B, the scl is also dissected away to reveal three large frontoturbinals (ft) within the frontal recess. C-F) Histological sections in the frontal recess of *Dasyprocta cristata*. C, a histological section through the rostral, free projections of frontoturbinals 2 and 3, also emphasized the greatly elongated and sickle-shaped scl (dashed line in A indicates a likely comparable cross-sectional level in *D. leporina*). At rostral levels, the scl and each ft is covered with pseudostratified, columnar ciliated epithelium (D, showing scl) or simple cuboidal/columnar, ciliated epithelium (e, showing ft2). F) ft3 has the most rostrally projecting olfactory epithelium (oe). bg, Bowman's glands. re, respiratory epithelium; s, septal cartilage; vs, venous sinus. Scale bars: A, 3 mm; B, 2.5 mm; C, 1 mm; D, 50 μm; E, 10 μm; F, 20 μm.

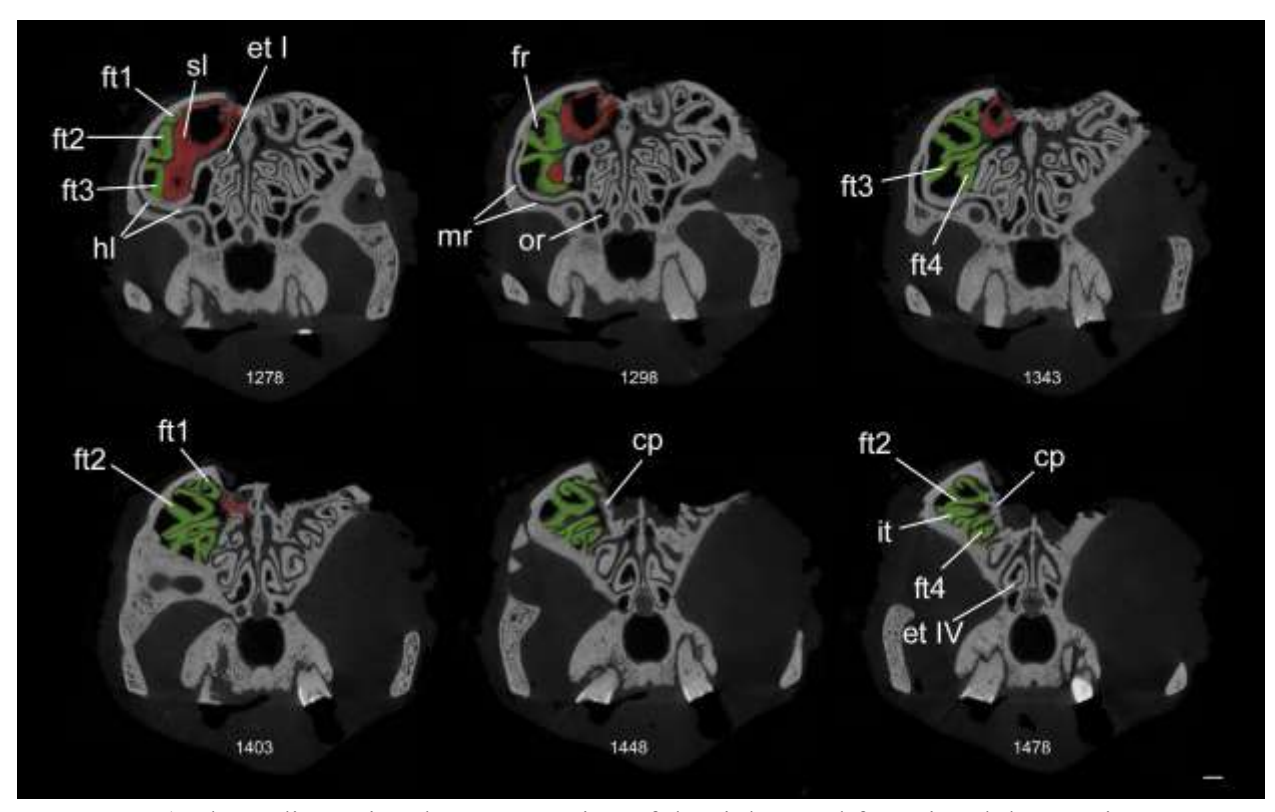


Figure 7. A) Three-dimensional reconstruction of the right nasal fossa in adult agouti (*Dasyprocta leporina*), with a dashed line indicating a cross-sectional level within the olfactory recess at the level of the first and second ethmoturbinals (etI and etII, respectively). A histological section at a similar level from a second specimen (*Dasyprocta cristata*) is shown in B). Here, a thick olfactory mucosa is found along adjacent surfaces of the semicircular lamina (scl) and septum (s), as well as the dorsal part of ET I. Note that little olfactory mucosa extends rostral to this point (see A, where the estimated distribution of olfactory epithelium is indicated in green). Bottom row: enlarged views of mucosa of the scl (C), etI (D), and septum (E). Note thick olfactory epithelium (oe) overlaying a deep lamina propria that includes numerous olfactory nerve bundles (on). Scale bars: a, 3 mm; b, 1 mm; c-e, 30 μm.

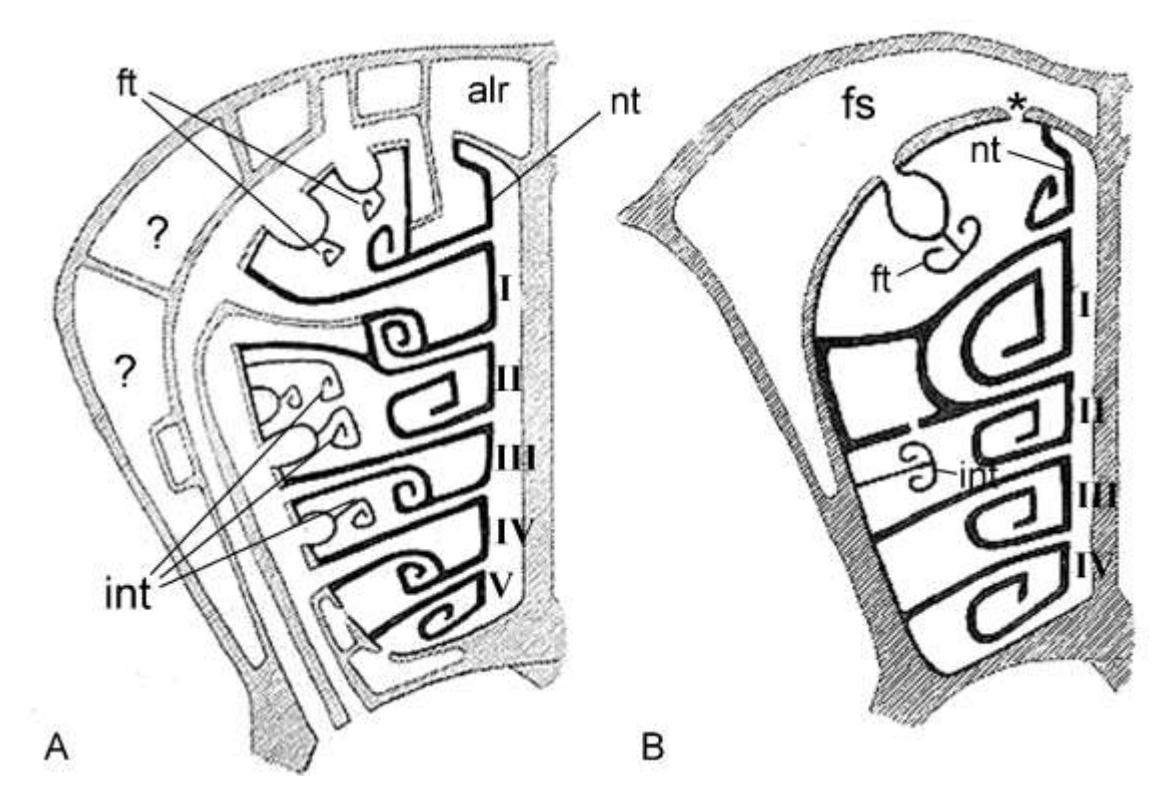
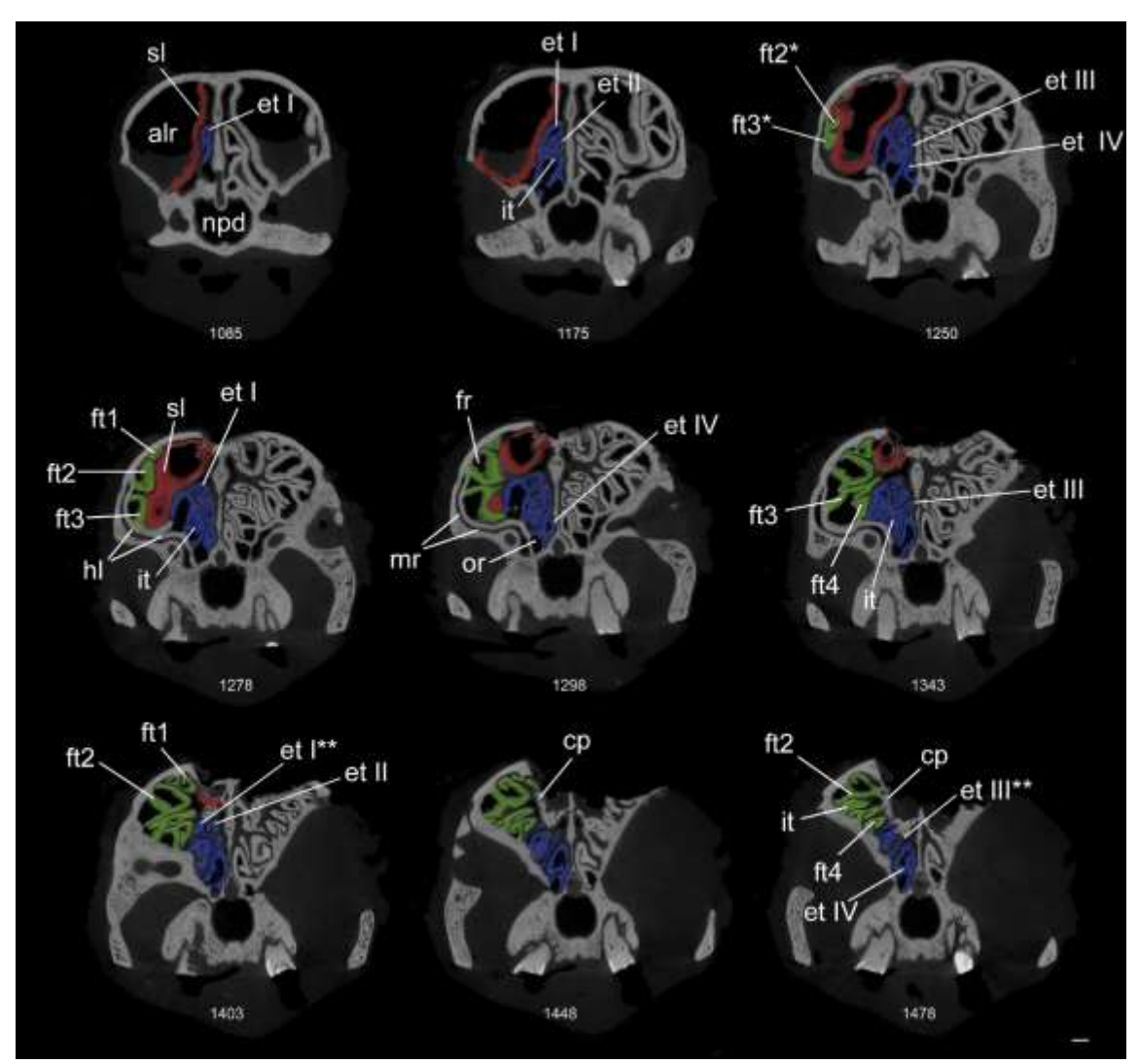


Figure 8. Redrawn and relabeled from Paulli (1900). Cross-sections, in downwardly leaning frontal planes (see Maier and Ruf, 2014, for further information) through the ethmoturbinal region of the nasal cavity of *Hystrix cristata* (A) and *Hydrochoerus hydrochoerus* (B). Turbinals and recesses are labeled according to the terminology used in this paper. *Hystrix* may have more turbinals overall than any other rodent. *Hydrochoerus* is notable for the advanced degree of pneumatization. fs, frontal sinus; ft, frontoturbinal; it, interturbinal; scl, semicircular lamina; I, II, III, IV, V, ethmoturbinals I to V; ? pneumatic expansions of uncertain homology.



Supplemental Figure 1: An extended series of rostral to caudal CT slices of *Dasyprocta leporine* is shown, to show a greater extent of the olfactory recess (numbers indicate rostrocaudal CT slice level). The semicircular lamina is tinted red; frontoturbinals are tinted green; ethmoturbinals and the interturbinal are tinted blue. Slice 1085 is near the rostral-most level of the olfactory recess (or), and space bordered by large bilateral anterolateral recesses (alr). Here, a plate of bone, the transverse lamina (tl) separates the olfactory recess from the nasopharyngeal duct (npd, the space ventral to the latter). The ethmotrubinals (et I, II, III, IV) and frontoturbinals (ft1, 2, 3) gradually become more complex in more caudal slices. An interturbinal (it) is observed among ethmoturbinals (e.g., 1278, 1343), as is common in mammals. An interturbinal (provisionally identified) is also observed among frontoturbinals (1478). The semicircular lamina (sl) is exceedingly elongated rostrally (1085 tp 1250). As this lamina reduces in extent caudally, the frontal recess (fr) expands (1278 to 1403). Ventral to the horizontal lamina (hl), the maxillary recess (mr) is a greatly compressed space (e.g., 1278, 1298). Very caudally, ethmoturbinal make connections to the cribriform plate (cp) with their more dorsal lamellae (examples indicated by **). Scale bar: 3 mm.

Table 1: Terminology for structures and spaces of the nasal fossa.

Structure name	Comments ¹		
Structures			
Nasoturbinal	Synonyms: dorsal nasal concha, pars rostralis (NAV²); endoturbinal I (Moore, 1981, fig. 84)		
Maxilloturbinal	Synonyms: concha ventralis (NAV); maxilloturbinate (Harkema et al., 2012)		
Ethmoturbinal I	Synonyms: concha media (NAV); ethmoturbinal II (Martin, 1990); endoturbinal II, upper lamella (Paulli, 1901; Moore, 1981); endoturbinal I (Allen, 1882)		
Ethmoturbinal II	Synonyms: concha ethmoidalis (NAV); ethmoturbinal III (Martin, 1990); endoturbinal II, lower lamella (Paulli, 1901; Moore, 1981); ethmoturbinal I, ventral lamella (Maier, 1993a)		
Ethmoturbinal III	Synonyms: concha ethmoidalis (NAV); ethmoturbinal IV (Martin, 1990); endoturbinal II (Paulli, 1900; Moore, 1981)		
Ethmoturbinal IV	Synonyms: concha ethmoidalis(NAV); ethmoturbinal V (Martin, 1990); endoturbinal III (Moore, 1981)		

Semicircular lamina Synonyms: semicircular crest; dorsal nasal concha, pars caudalis (NAV)

Frontoturbinal Synonyms: ectoturbinal (Paulli, 1901; Moore, 1981)

Frontomaxillary septum Synonyms: lateral root of ethmoturbinal I (Rossie, 2006); anterior root of ethmoturbinal I (de Beer, 1937); horizontal lamina (Maier, 1993a)

Interturbinal (Maier, 1993b) Synonyms: ectoturbinal (Paulli, 1900; Moore, 1981); accessory turbinal (Dieleux, 1906)

Transverse lamina synonyms: lamina terminalis (Kollmann and Papin, 1925; Hill, 1953); posterior transverse lamina (Macrini, 2012)

Spaces

Anterolateral recess Term first used by Smith and Rossie (2008) to refer to the rostral part of the recess that is lateral to the

semicircular crest; caudally, it merges with the frontal and maxillary recesses; synonyms: recessus anterior (de

Beer, 1937); maxillary sinus (Rowe et al., 2005, see figure 5 therein)

Posterolateral recess This is equivalent to both the frontal and maxillary recesses, together (Adams and McFarland, 1972)

Frontal recess Synonyms: superior maxillary recess (Negus, 1958, p 313)

Maxillary recess	Synonyms: inferior maxillary recess (Negus, 1958, p 313); postnatal: maxillary sinus ³
Olfactory recess	Synonyms: sphenoethmoidal recess; ethmoturbinal recess (Maier, 1993a); cupular recess (van Gilse, 1927); sphenoidal recess (Loo, 1973)

¹See Moore (1981) and Smith and Rossie (2006, 2008) for further discussion; ²NAV (Nomina Anatomica Veterinaria); ³ the maxillary sinus, technically, results from pneumatic expansion beyond the limits of the fetal maxillary recess in humans.

Table 2: Notes on rostrocaudal identity of epithelial type on each of the turbinals in the main nasal chamber and frontal recess.

Region	Olfactory epithelium?	Notes
Central chamber		
Ethmoturbinal I	Present	No OE for most rostral 1.3 mm of the turbinal; first patch of OE found medially, then laterally as well; at 1.8 mm from the rostral tip OE is also found dorsally.
Ethmoturbinal II	Present	First patch of OE found medially, 1.44 mm from the rostral tip.
Ethmoturbinal III	Present	OE present but poorly preserved rostrally.
Ethmoturbinal IV	Present	OE present but poorly preserved rostrally.
Interturbinal (between ET II and ET III)	Present	OE present but poorly preserved rostrally.
Nasoturbinal	Absent	No OE anywhere along its rostrocaudal length.
Semicircular lamina	Present	This bears the most rostrally positioned olfactory epithelium of any nasal cavity structure.
Frontal recess		
Frontoturbinal 1	Present	OE present but poorly preserved rostrally.
Frontoturbinal 2	Present	The most rostral 2.5 mm is devoid of OE; the first small patches face medially
Frontoturbinal 3	Present	This turbinal has the most rostrally positioned OE of all the frontoturbinals; most rostral 1.8 of turbinal is devoid of OE.
Frontoturbinal 4	Present	OE present but artefactual folding of some more rostral sections hinder determination of how far rostrally it extends.
Interturbinal (between frontoturbinals 3 and 4)	?	Mucosa poorly preserved.